A PHYSICAL ASSESSMENT OF SNAKE POND OF CAPE COD, MASSACHUSETTS, INCLUDING A THERMAL AND SURFACE/GROUND WATER MODEL

by

RONALD SANG LEE

B.S. Environmental Engineering
Columbia University, 1996

Submitted to the Department of Civil and Environmental Engineering
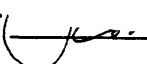In Partial Fulfillment of the Requirements for the Degree of

MASTER OF ENGINEERING
IN CIVIL AND ENVIRONMENTAL ENGINEERING

at the

MASSACHUSETTS INSTITUTE OF TECHNOLOGY
June 1997

© 1997 Ronald Sang Lee

The author hereby grants to M.I.T. permission to reproduce and distribute publicly paper and electronic copies of this thesis document in whole or in part.

Signature of the Author _____
Department of Civil and Environmental Engineering
May 9, 1997

Certified by _____
Advisor
Lecture Professor/Professor of
Civil and Environmental Engineering
Thesis Supervisor

Accepted by _____
Professor Joseph Sussman
Chairman, Department Committee on Graduate Studies

A PHYSICAL ASSESSMENT OF SNAKE POND OF CAPE COD, MASSACHUSETTS, INCLUDING A THERMAL AND SURFACE/GROUND WATER MODEL

by

RONALD SANG LEE

Submitted to the Department of Civil and Environmental Engineering
on May 10, 1996 in Partial Fulfillment of the Requirements for the
Degree of Master of Engineering in Civil and Environmental Engineering

ABSTRACT

This study uses a number of computer models to examine the flow of water into and inside Snake Pond, a kettle-hole pond in Cape Cod, Massachusetts. Next to the pond are a set of injection and extraction wells which are containing a contaminant plume originating from the Massachusetts Military Reservation. The effects of the wells on the water table were simulated using two different two-dimensional models, one in plan view and one in elevation. From this, it was determined that all the water originating from wells upgradient of the pond will enter the pond. This will comprise of between 40-70% of the groundwater entering Snake Pond. Another model was developed to determine the thermal structure of the pond. This model requires only bathymetry, meteorological data, and an extinction coefficient to calculate the temperature profile of a small freshwater pond with no significant surface water inflows or outflows. From this model, it was determined that Snake Pond may be considered a well-mixed tank, that it is insensitive to changes in the extinction coefficient, and that wind is the dominant mixing mechanism in Snake Pond.

Thesis Advisor :   Harold F. Hemond

Title   :   Professor of Environmental Engineering, Director of Parsons Laboratory

Acknowledgements

The author of this thesis, finishing under threat of an extra year at MIT, wholeheartedly acknowledges and shares liability with the following people who have helped him become a Master:

Bob Davis, who finagled data when no one would have thought it possible.

Jackie Donoghue and **Muriel Frederick**, who kept an eye out for the author's very important package and caught it just in time.

Eric Adams, who, with his extraordinary finesse in modeling problems, helped the author see intuitively many concepts he would not have otherwise.

Bruce Jacobs and **Peter Shanahan**, the project advisors, who provided motivation and support in the author's dreary and unproductive winter months.

David Marks, who helped shape the direction of the author's academic career and tolerated the author's annoying pleas for money.

Yervant Vichabian, Jacques De Lalaing, Dan Baker, and **David Lockwood**, fellow members of the FS-12 project team, without whose company and commiseration the author would have felt very behind indeed.

Scott Goddard, fellow Snake Ponder, who made the author feel very behind indeed, and provided motivation for the author to get moving. Special thanks to Scott for allowing the author to continually beat him at cards.

and **Harry Hemond**, a really great guy, who made time for the author even at his busiest moments. His patient explanations and keen eye kept the author on his toes and helped shape the thesis into what it is today.

TABLE OF CONTENTS

TABLE OF FIGURES

1. Overview

1.1 The Problem

Fuel Spill 12 (FS-12) is one of several groundwater plumes emanating from the Massachusetts Military Reservation (MMR) on Cape Cod. Over the years, the MMR has been occupied by several military organizations, and was particularly active during World War II. During its 86 years of operation, the MMR has been home to a number of pollution incidents, and was declared a Superfund site in 1990.

FS-12 plume was caused by approximately 70,000 gallons of jet fuel that leaked from an underground pipeline. It was discovered in 1990. Whereas the leak occurred on the reservation, the majority of the plumes reside just outside the MMR perimeter. The contaminants of the fuel spill include benzene and ethylene dibromide (EDB), both of which are known carcinogens. This plume pose no immediate threat to Cape Cod water resources. However, the increasing population, as well as the region's dependence on groundwater and the continuing growth of the plume, have concerned many scientists and members of the surrounding communities.

A wide range of chemicals are present in the plume, each moving at a different velocity. The two chemicals of greatest concern are benzene and EDB, and the flow of these may be thought of as two separate plumes. These two plumes are distinct in position and composition, and are joined together only at the source. The benzene plume moves along the surface of the groundwater. Air sparging wells and soil vapor extraction units have been remediating the benzene plume since 1995. The EDB plume starts near the surface but sinks downgradient. The tail of the plume is 140ft or more below the ground surface, and is traveling downgradient faster than the benzene plume. Currently, no remediation schemes have been developed for this plume; however, the Installation Restoration Program (IRP) plans to have an extraction/treatment/reinjection (ETR) system in operation by the summer of 1997. This system has been designed to trap a large percent of downgradient EDB with minimal impact to the

environment. However, there has been some concern about the effects that the pump and treat system will have on Snake Pond, a small kettle-hole pond bordering the EDB plume along the southwest edge, next to which a number of reinjection wells will be placed. Groundwater models predict that a large quantity of injected water will enter the pond and may significantly alter the chemistry and ecology of the pond.

1.2 The Scope

This study is an effort to better characterize water flow associated with Snake Pond and to provide a clearer understanding of the movement of water injected by the ETR system. Flow of injected water in both the ground and the pond has been studied. In this report, the following tasks are described:

- An evaluation of existing groundwater models of FS-12 and Snake Pond,
- The implementation of an analytical surface/ground water model,
- A calculation of treated water entering Snake Pond,
- The development and implementation of a thermal model,
- A test of the validity of the model,
- A model run on Snake Pond, and
- An analysis of the impacts of the model variables on mixing mechanisms at Snake Pond..

2. Site Description

2.1 Physical Characteristics

2.1.1 Location

The Massachusetts Military Reservation (MMR) is located in western Cape Cod, Massachusetts, and is bordered by the townships of Bourne, Falmouth, Mashpee, and Sandwich (Figure 2-1). A number of U.S. military organizations are housed at the reservation, including the Coast Guard, Marine Corps, Army National Guard, Air Force, and Air National Guard. Other portions of the base are used by the Veterans Administration National Cemetery, the U.S. Department of Agriculture, and the Commonwealth of Massachusetts. The southern portion of the reservation contains most of the facilities, while the northern portion is composed mainly of firing ranges (Advanced Sciences, 1993).

2.1.2 Topography and Geology

Western Cape Cod is characterized by rolling hills, broad areas of low relief, and marshy lowlands. Most of the MMR and all of the FS-12 site lie in a broad glacial outwash plain called the Mashpee pitted plain (MPP). The MPP is noted for low topographic relief and for an abundance of kettle hole ponds and marshes. A zone of surface soil and weathered residues covers the MPP, and ranges between two to five feet in depth. This soil consists of silty clay or clayey silt, with variable mixtures of fine sand and/or organic matter. Under this layer are outwash sand and gravel, interspersed with a few lenses of lower permeability, fine grained sand, silt and clay. The gravel component typically ranges between 0 to 25 percent, though larger percents are common in the uppermost 30 ft. This sand is predominantly quartz and feldspar, with surface coatings of iron oxide and some manganese oxide. This outwash extends at least 130 ft below the water table. Below this, there are intervals of fine grained sediments,

9
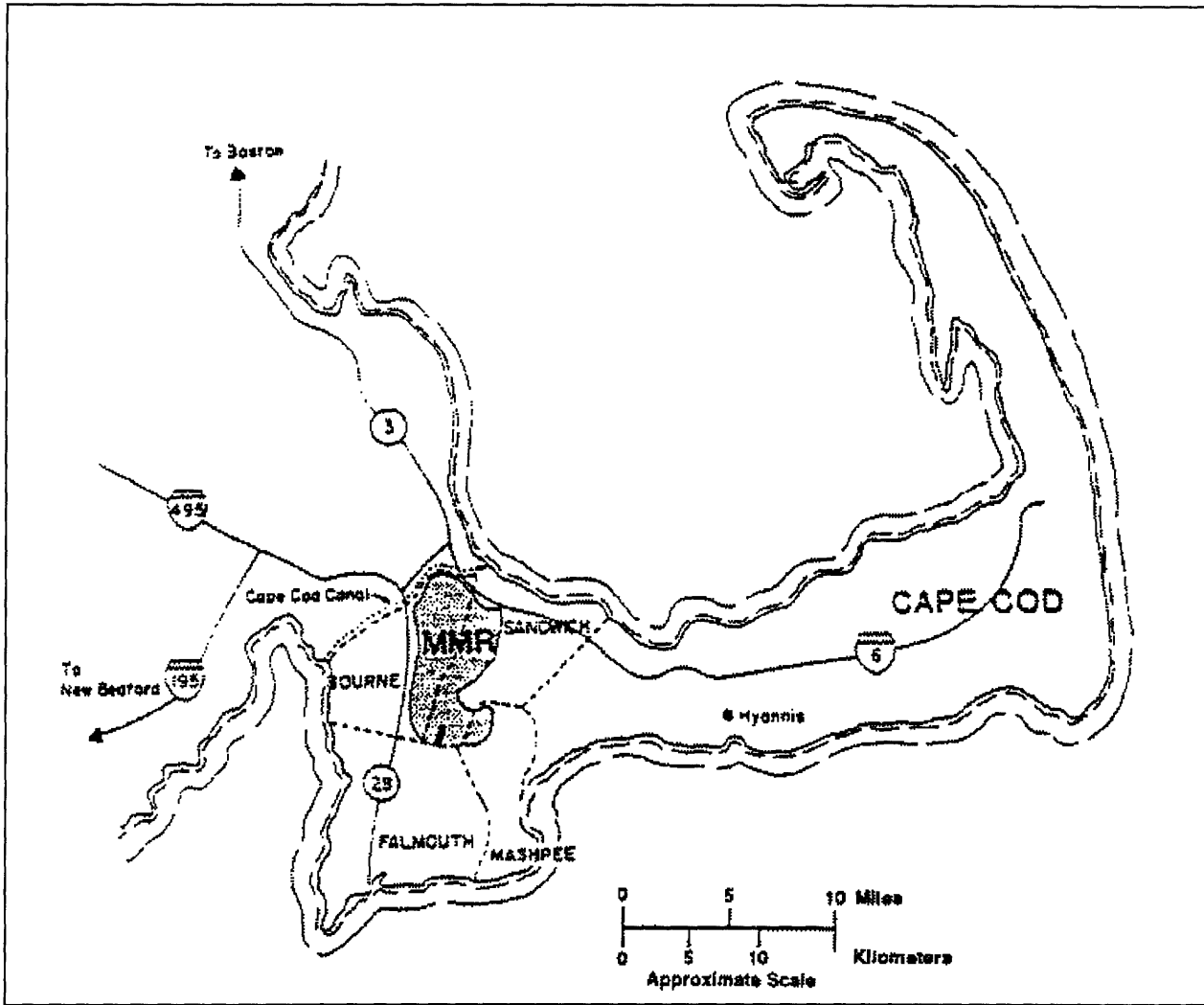
Figure 2-1: Location of the MMR

extending to a depth of 215 ft. Very few deep hole borings have been made, so thickness data for these intervals are limited. Engineers have not drilled to the bottom of the aquifer, but seismic surveys indicate that there is a confining layer of bedrock (Knoll et al., 1991).

The northern and western sides of the MMR lie in a terminal moraine—irregular, hilly terrain with greater topographic relief. The sediments of these moraines are mixtures of till, sand, silt, clay, and gravel to boulder size clasts. The MMR has an elevation high of 306 feet, at Pine Hill in the west-central portion of the MMR, a low of 0 feet at sea level.

2.1.3 Snake Pond

Snake Pond is a small kettle-hole pond that borders the FS-12 plume on the southwest side. Being a kettle-hole, it has no significant surface inflows or outflows, and the water in the pond is part of the groundwater table that has surfaced. Snake Pond is surrounded by woods, with some residential development to the south and a summer day-camp to the northeast. The pond has a surface area of 83 acres and a maximum depth of 31 feet.

2.1.4 Hydrogeology

FS-12 is located above the Cape Cod Aquifer, an unconfined aquifer covering a good portion of western Cape Cod (Figure 2-2). The total thickness of the saturated zone is estimated to be in excess of 200 ft, with an average depth` to water of 70 ft. The water table is exposed at the surface in Snake Pond, located at the southwestern boundary of the EDB plume. Data indicate horizontal gradients in the range of 0.0003 to 0.00067 ft/ft to the south-southeast. This range is one order of magnitude lower than gradients in adjacent areas of the MMR. The area has an estimated horizontal hydraulic conductivity of 151 ft/day, an estimated porosity of 30 percent, and a horizontal flow velocity of 0.15ft/day.

2.1.5 Regional Climate

Cape Cod has a temperate climate, with expected annual temperatures ranging from 19 to 81 degrees Fahrenheit. Temperatures remain fairly moderate due to the proximity to the Atlantic Ocean and the accompanying Gulf Stream. Wind speeds typically vary from 9 to 12 miles per hour with stronger storm velocities of 40 to 100 mph. Annual precipitation averages 45 inches with a somewhat higher portion in winter than summer. Annual groundwater recharge is in the range of 26 inches/year. The one-year/24-hour rainfall event measures 2.7 inches (Advanced Sciences, 1993).
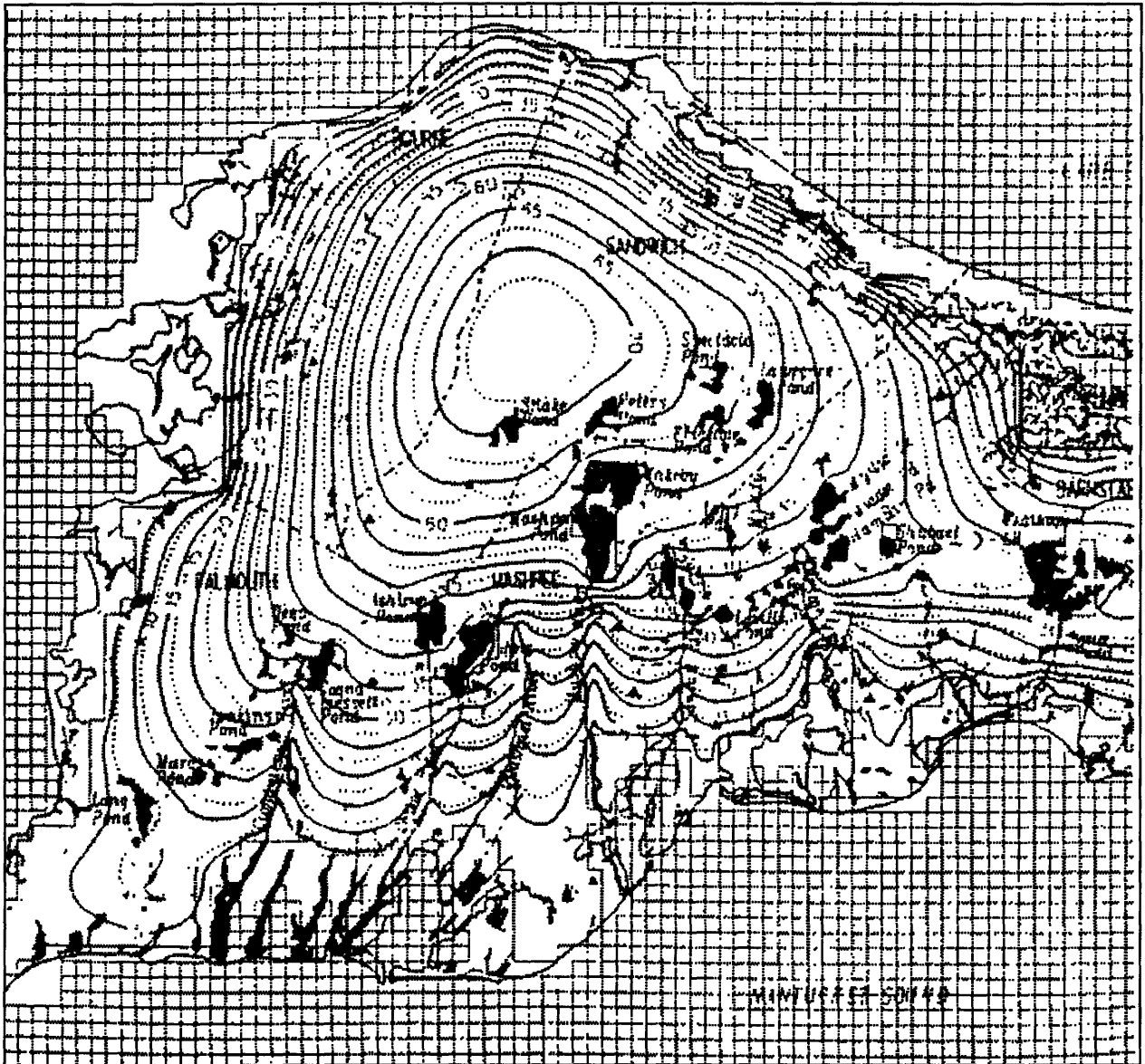
Figure 2-2: The Cape Cod Aquifer

2.1.6 Ecosystems

The coastal plain ponds, formed in the glacial kettles of Cape Cod, are considered unique and sensitive natural communities by the Massachusetts Division of Fisheries and Wildlife. The rare ecosystem that develops on the shores of these ponds is highly sensitive to water level, temperature, and pH changes.

2.2 Demographics and Socio-Economic Impacts

The Fuel Spill-12 plume is located on the Upper Cape, near the top of the Sagamore lens. Being the sole-source water-supply aquifer for western Cape Cod, the lens is of vital importance to the four towns adjacent to the MMR - Falmouth, Mashpee, Sandwich, and Bourne (Ryan, 1980).

The MMR has a year round population of approximately 2,000 people with an additional 800 nonresident employees. The population of the four surrounding towns fluctuates greatly between winter (29,000) and summer (70,000) due to a strong tourism industry. Between 1980 and 1990, the Upper Cape population grew 35%. In comparison, the population growth of Massachusetts was 5% over the same period.

In the Upper Cape, 80% of the population relies on a public water supply system, while the remaining 20% rely entirely on private wells for their water supply. The average demand during the off-season is 8 million gallons per day (MGD), but can reach as much as 16 MGD during the summer (Bosch et al. 1996).

3. Fuel Spill 12 Background

3.1 Pollution History and Regulation

The MMR has been used heavily by many military organizations since its inception in the 1910's. The heaviest activity was between 1940 and 1946 by the U.S. Army, and from 1955 to 1972 by the Air Force. During these years, it was common practice to dispose of such wastes in landfills, drywells, to burn them at firefighter training areas, or simply to dump them wherever was convenient. Some of these products worked their way into the groundwater and went unnoticed for years. In 1978, the Town of Falmouth detected detergents in a municipal drinking water supply well 7,500ft south of the base boundary. The detergents were later traced back to the base's wastewater treatment plant. In 1982, the Installation Restoration Program (IRP) was initiated by the Department of Defense to investigate and clean up environmental problems at the MMR. To date, 79 sites have been identified as having the potential for environmental problems (Figure 3-1) (MMR, April 1996).

FS-12 was believed to have started in 1972 by a bulldozer breaking a three-inch pipeline which ran from Cape Cod Canal to the base. This breach was not realized by the pipeline operators, who continued to send JP-4 jet fuel through the pipeline. As many as 70,000 gallons poured into the ground, creating a puddle of free floating product and a plume that, as of May 1997, is 4,800 feet long, 2,750 feet wide, as much as 130 ft thick, and 100 to 240 feet below the ground surface. The FS-12 plume was discovered in 1990 by engineers who performed exploratory drilling for municipal supply wells. Groundwater sampling and analysis by the Sandwich Water District indicated concentrations of volatile organic compounds, predominantly benzene (Advanced Sciences, 1993). Subsequent investigations indicated that the groundwater was contaminated primarily with dissolved phase benzene, toluene, ethylbenzene, and xylenes (BTEX), and EDB, which the EPA lists as a probable human carcinogen. 1.5 billion gallons of water have been contaminated, and the plume is moving south toward Snake Pond and a public water supply well in Sandwich (Rolbein, 1995).

14

The MMR was listed as a Superfund site on the National Priority List on November 21, 1989. The National Guard Bureau (NGB) and the U.S. Coast Guard entered into an Interagency Agreement (IAG) with the EPA in July 1991. As a result, the site investigation and remedial action are subject to the requirements and regulations of the Comprehensive Environmental Response and Emergency and Liability Act (CERCLA) (Bosch et al. 1996).

3.2 Plume Treatment

As of May 1997, two systems are removing fuel at the source of FS-12: an air sparging (AS) system and a soil vapor extraction (SVE) system. The SVE extracts air from the vadose zone via a vacuum pump. The high volatility of organic compounds allows the SVE remove the gasoline vapors above the free floating product. The AS injects air into the saturated zone. As the air moves upward and comes in contact with free or dissolved fuel, it strips the water of contaminants and free product. When the air reaches the vadose zone, it is extracted by the SVE system. The AS also promotes biodegradation by providing oxygen to fuel-eating bacteria. The SVE system began operation on October 23, 1995, and the AS system began on February 21, 1996. By September 1996, about 39,100 pounds of product had been removed from the site (MMR, December 1996).

As of May 1997, an extraction/treatment/reinjection (ETR) system is being constructed to contain the plume. The system will consist of 30 extraction wells, 23 reinjection wells, and a treatment plant for the extracted water (Figure 3-2). For ease of reference, the wells have been subdivided into three groups: the two northernmost wells, called the northern injection wells, six wells on the southwest side, called the central injection wells, and the remaining 15 wells along the south and southeast, called the southern injection wells. The ETR will draw water out of the aquifer and remove the fuel compounds by running the water through activated carbon canisters. The carbon adsorbs the fuel compounds and the treated water is reinjected to the ground. The carbon canisters are recycled off-site periodically. Construction of the ETR started in November 1996, and is scheduled to start operating in August 1997 (MMR, December 1996).
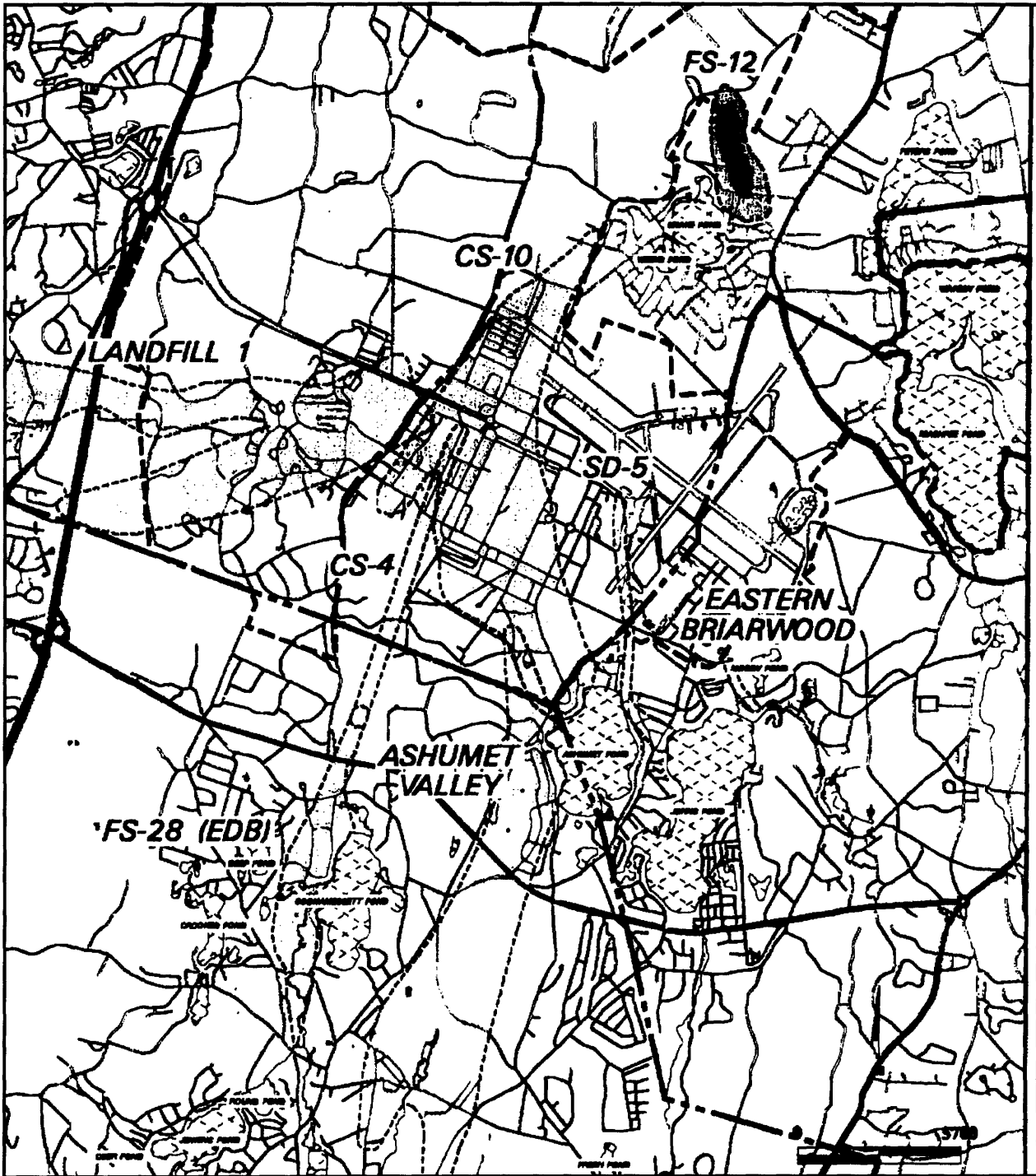
Figure 3-1: Map of MMR Plumes (Feb. 1997)

3.3 Potential Contaminants of Snake Pond

There are three "contaminants" of concern that may flow into Snake Pond: benzene, EDB, and reinjected water from the ETR. Of these, only the reinjected water is expected to enter the pond in any significant quantities. Models of these contaminants flows are discussed in this section.

The benzene plume travels near the surface of the ground water, and could cause significant damage to the environment if it reached Snake Pond. Triantopoulos (1996) used a computer model to examine the effects of the benzene plume on Snake Pond, without the ETR in operation. Using the groundwater model DYNFLOW, Triantopoulos modeled benzene as conservative particles, and the lake as a region of very high hydraulic conductivity. The particles were tracked over a model run of twenty years. By counting the number of particles entering Snake Pond and accounting for volatility of benzene in groundwater as first-order decay, the mass flux of benzene into Snake Pond was calculated. Assuming that the pond behaved as a well mixed tank, that benzene volitilization at the surface behaved as first-order decay, and that the flux of groundwater, rain water, and evaporation into and out of the lake were constant, Triantopoulos calculated the expected benzene concentration in the lake. As a very conservative estimate, the concentration is not expected to reach above 0.3 mg/L up to the year 2016. This value is about 8 times less than the concentration that would result in the threshold risk level to humans, defined by the Massachusetts Contingency Plan (Automated Sciences Group, Inc., 1994). So the benzene plume is not expected to significantly affect Snake Pond for some time.

Without the ETR in operation, Advanced Sciences (1995) predicted that groundwater will not travel from its current depth (about 140ft or more below the ground surface) upward to the ground surface or to surface-water bodies such as Snake Pond. Because of the extreme depth of the contaminant plume, no ecological exposures and therefore no ecological risk from the EDB was to be expected. P-Squared Technologies (P2T) and Jacobs Engineering performed a groundwater model to predict the flow of water (Jacobs, 1996). In this model, dilution and attenuation were assumed negligible, EDB was assumed to move without retardation, and the pond was assumed to be a region of very high conductivity. P2T ran the model to predict flow

for when the wells were operating and when they were not. No significant mass of EDB flowed into Snake Pond in either scenario, but they predict that about 70% of the groundwater flow into Snake Pond will be from the reinjection wells.

The USGS has also prepared a model to predict the influence of the ETR on the groundwater flow. They have used a program called BRAC-3D, and their model is similar in many respects to the Jacobs model. They have also predicted a treated water inflow of about 70%.

Concerns over the amount of plume that will be captured by the ETR, as well as potential impacts to the water level of Snake Pond have prompted the IRP to change their well configuration several times. For this study, I have used data from scenario 58. The configuration of wells is shown in Figure 3-2, and the pumping rates in Table 4-2.
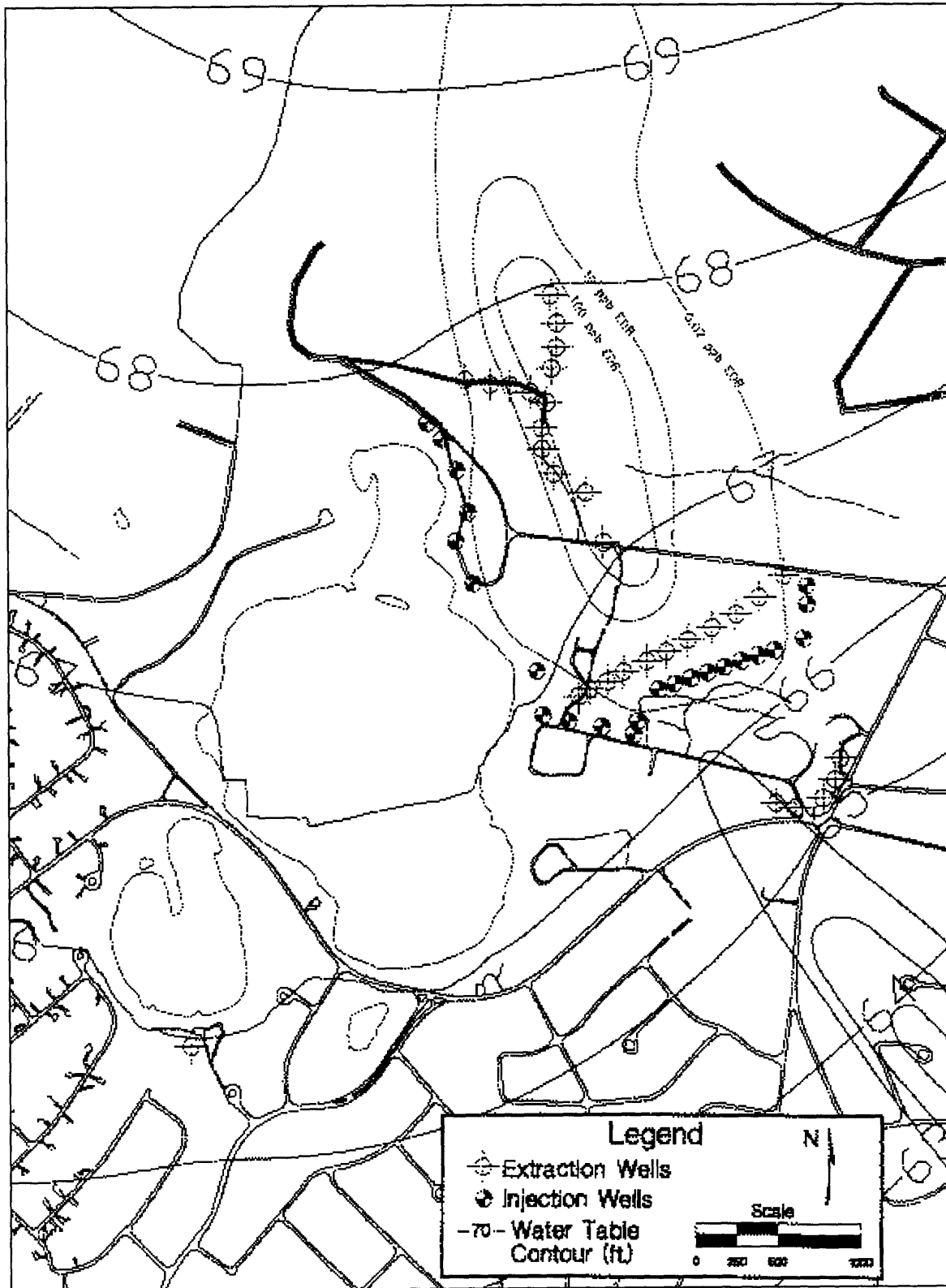
Figure 3-2: Map of ETR system

4. Water Flow into Snake Pond

4.1 Surface/Ground Water Modeling Background

Knowledge of groundwater flow into lakes has evolved from two different directions. One direction of attack, developed by watershed hydrologists, deals with subsurface water flowing through macropores in the unsaturated zone due to precipitation-runoff that infiltrates the ground. This flow is important where lakes are surrounded by steep forested hill slopes. Since the flow is a function of parameters that are difficult to measure, such as land topography, soil porosity, and intensity of precipitation events, it is hard to model explicitly. Models often account for this flow as part of a lumped parameter.

The other realm of study has been the flow of water in the saturated zone, developed by hydrologists. Groundwater flows into and out of lakes due to head gradients. The study of this interaction has been greatly based on discretized groundwater models. Because groundwater and surface water have such an extensive interface, their interactions have been the interest of study for over 100 years.

The equation commonly used to describe groundwater flow in heterogeneous and anisotropic porous media is a combination of the continuity equation and Darcy's equation:

$$\frac{\partial}{\partial x}(K_{xx}\frac{\partial h}{\partial x}) + \frac{\partial}{\partial y}(K_{yy}\frac{\partial h}{\partial y}) + \frac{\partial}{\partial z}(K_{zz}\frac{\partial h}{\partial z}) - W = S_s\frac{\partial h}{\partial t} \qquad \text{Eq. 4-1}$$

where

$x, y, z =$ Cartesian coordinates aligned with the principal axes of K

$K_{jj} =$ Hydraulic conductivity in the j-direction

$h =$ Potentiometric head

$W =$ Volumetric flux per volume (sources or sinks of water)

S_s =   Specific Storativity

t   =   time

A number of models have been created to better understand the mechanics of the surface/ground water interaction. The steady state form of equation 4-1, with W and t equal to zero, has been examined by Toth (1963). After solving the equation analytically, he evaluated flow configurations caused by different water-table conditions in two-dimensional flow. The two dimensional assumption is valid for lake shores and ground-water divides that are straight, parallel, and infinitely long (Lerman et al). Simulating the water table as a sine wave, Toth found that there were several flow systems working at different magnitudes, and the flow patterns were strongly dependent on the water table configuration.

Winter (1976) has developed models to examine the effects of hydrogeology, topographic and water table elevation, lake depth, the number of dimensions modeled, and recharge rates for small lakes. Like Toth, Winter analyzed flow for two-dimensional steady state flow. The water table was configured such that there were mounds on both sides of the lake, with one water table mound being higher than the other. Under these conditions, he found that water always flowed into the lake along the upper part of the groundwater table, though water could flow outward from the lake through deeper parts. The mounds create small local flow cells beneath themselves from which groundwater discharges into the lake. Both the mound and the local flow cell can be ephemeral in an unsteady system (Winter, 1983). During recharge events, the mound grows and the underlying flow cell expands, possibly large enough to prevent outseepage. After recharge stops, the mound dissipates and, after a period of time, allows water to flow out of the lake downgradient. Winter's simulations of unsteady conditions (1983) show that flow reversals on the downgradient side of the lake are dependent on the height of the groundwater mound and the local hydrogeologic conditions. In addition, he suggests that water quality within the local flow cell may differ considerably from that of the groundwater system. Cherkauer and Zager (1988) have made observations on the flow of water in small, fully penetrating kettle hole lakes in southeast Wisconsin. Using seepage meters and by measuring the concentrations of chloride

caused by septic and agricultural contamination, they found that the flow patters for these lakes were consistent with Winter's predictions.

McBride and Pfannkuch (1975), also working with equation 4-1, developed a two-dimensional model to determine how seepage is distributed over the bottoms of natural lakes. Among their assumptions are that the aquifer modeled has an impermeable lower boundary, that the soil is heterogeneous and isotropic, and that flow divides are straight and vertical, with the flow divide under the lake below the lake's center (assuming a reasonably symmetrical lake). Solving equation 4-1 numerically, their models shows that seepage of water into or out of lakes tends to be concentrated near the shores, and decreases exponentially with distance from the shore. Field observations by Lee (1977) and Pfannkuch and Winter (1984) support their conclusions for lakes whose widths are at least 1/3rd the thickness of the aquifer. However, Cherkauer and Nader (1988), taking data from the Great Lakes, have found that hydraulic heterogeneities in large systems cause seepage patters which differ considerably from the simulated results.

4.2 Data Available

Some of the data used in this chapter comes from an aquifer injection test, in which water was pumped both into and out of sites close to the FS-12 (Optech, October 1996). By taking readings from a number of observation wells near these pumping/reinjection wells and applying Theis and Neuman method solutions, values for transmissivity, hydraulic conductivity, and storativity were derived. However, the fit of most of the data to type curves were fair to poor, and the many of the hydraulic parameters derived from this test are suspect. However, some data, such as the hydraulic conductivities, ambient conditions of the groundwater table, and the maximum drawdown during steady state pumping, have been deemed reliable for this present study.

Very little has been done to determine the characteristics of the groundwater flow near Snake Pond. Seepage meters were installed into Snake Pond in May 1996. These meters are essentially barrels with the open end inserted into the lake bed. On the other side of the barrel,

an expandable bag is attached to a punched hole, into which groundwater can flow. Seepage rate is measured as a function of the volume of water in the bag after a given time. At the time of this report, the data was still being obtained and was unavailable. However, even with data from seepage meters, it is hard to get a clear picture of the interaction of lakes with subsurface water. Besides uncertainties in the actual measurement of seepage, the distribution of seepage is not uniform, due to the heterogeneity of lake beds, transpiration from near-shore vegetation, and non-uniform bending of groundwater flow paths where the sloping groundwater table meets the flat lake surface (Lerman et al, 1995). Therefore, parameters such as quantity of groundwater flow into the lake have been taken from the results of the Jacobs and USGS groundwater models. The uncertainties mentioned for seepage meters also hold true for the groundwater models, which do not differentiate between flow characteristics close to and far from the pond.

4.3 Modeling

The modeling of the groundwater near Snake Pond has been divided into two efforts: a two-dimensional model that shows water behavior in elevation view, and a two-dimensional model that shows behavior in plan view. By putting the two together, it is possible to get some idea of the three-dimensional flow of water near Snake Pond.

4.3.1 Elevation View Modeling: The FlowThru Model

The FlowThru model was developed by Lloyd Townley (1992) to describe features of the surface water/groundwater interaction on the Swan Coastal Plain in Western Australia. In its database are a set of pre-calculated solutions, obtained using a linear triangular finite element model. Taking inputs from the user, FlowThru combines these solutions and can display the streamlines of water in elevation view, as well as the quantity of water entering along various sections of the surface water/groundwater interface.

4.3.2 Assumptions

Being two-dimensional, FlowThru is designed for use with long bodies of surface water which lie perpendicular to the direction of subsurface water flow, such as rivers or elongated lakes. Snake Pond does not fit this description well; its long direction lies parallel to groundwater flow. Moreover, since FlowThru calculates in two dimensions, it can only represent sections which are aligned with the direction of regional groundwater flow. The pond shore and the groundwater contours surrounding it are not very straight, making it even more problematic to determine an appropriate model length for the pond. For this reason, a range of pond lengths were used in this model. Figure 4-1 shows the streamlines calculated by the USGS model for scenario 58. Some of these lines start from the reinjection wells, make their way under the lake, and eventually exit. Since FlowThru requires aligning a modeled section with the groundwater flow, the length of these lines under the lake are a good measure for the pond length in the model. The shortest line shown on Figure 4-1 starts from the southernmost well among the north injection wells, and travels a length of 600 feet. The majority of the lines are over 2000 ft; therefore a pond length of 1600 ft, the maximum length that FlowThru allows for the aquifer underlying FS-12, was also used.

In modeling lakes as regions of constant head that lie along the groundwater table, FlowThru assumes that the water bodies are shallow relative to the thickness of the aquifer. Irregular boundaries are not considered; however, the length of the bottom may be used. For the sections of concern, this is not a concern, since the regions over which the short-streamline particles travel never reach the deeper southern region of Snake Pond.

FlowThru simulates flow in a rectangular domain, and the groundwater table is assumed to stay horizontal throughout. In reality, the groundwater does have a gradient, but since it is quite small (5.3×10^{-4} ft/ft at FS-12), the approximation is reasonable.

Flow Pathlines
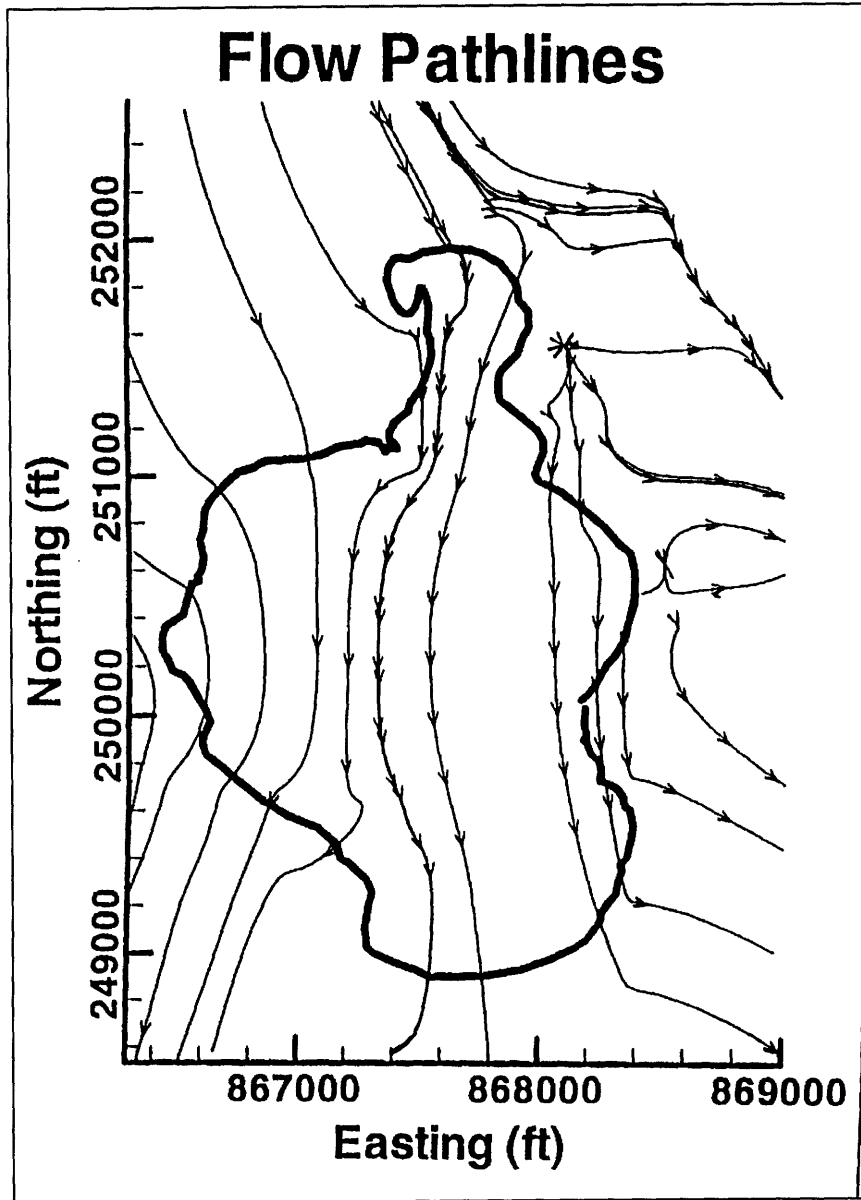
Figure 4-1: USGS Prediction of Flow Paths

Geometry of the modelled domain.

Fluxes through the boundaries of the modelled domain.
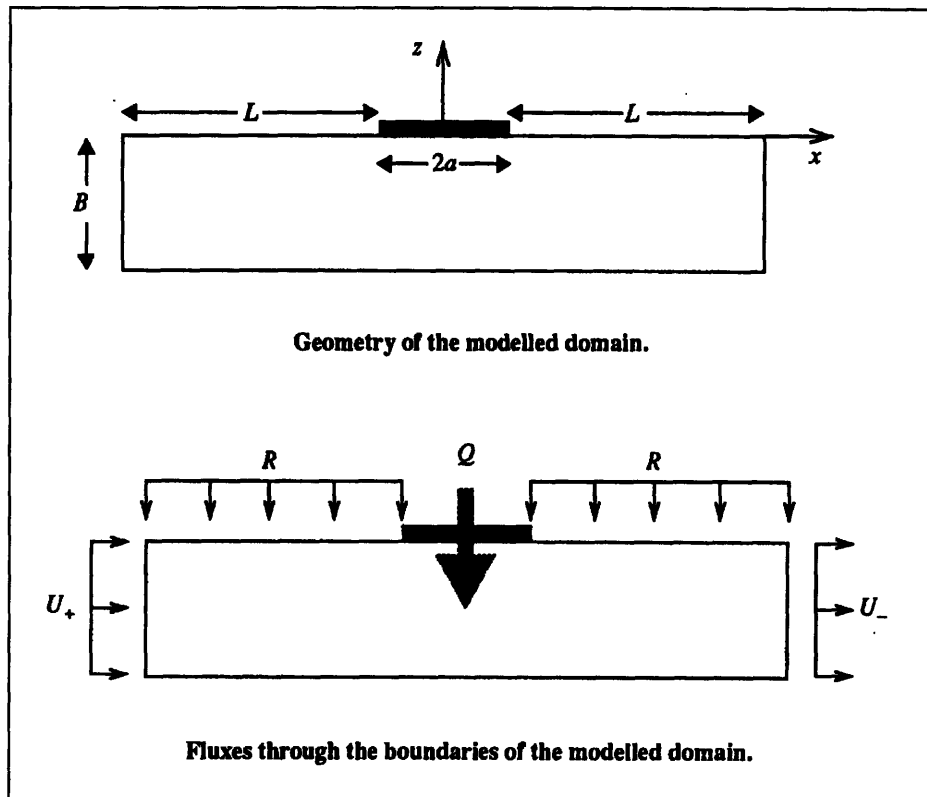
Figure 4-2: Schematic of FlowThru Inputs

4.3.3 Inputs

Figure 4-2 shows a the variables used by FlowThru. With the exception of Q and L, all variables are input by the user as dimensionless ratios. These ratios are: the groundwater flow out divided by the groundwater flow into the surface water body (U-/U+), the recharge rate divided by the groundwater inflow rate (RL/U+B), the anisotropy (K_x/K_z), the length of the surface water body divided by the thickness of the aquifer (2a/B), and the equivalent thickness due to sediment at the bottom of the surface water body divided by the thickness of the aquifer (D/B). Values for Q, net flow into the water body, and L, the length from the boundary of the model to the edge of the lake, are calculated by FlowThru based on these inputs. Q is calculated using conservation of mass:

$$Q = U_-B - U_+B - 2RL$$

and L is set at

$$L = 2B\sqrt{K_x / K_z}$$

The values used in this model are shown in Table 4-1.

Table 4-1: Inputs Used for FlowThru

Input	Run 1	Run 2	Run 3
U-/U+	1	1	2
RL/U+B	0.14	0.14	0.14
K_x/K_z	3	3	3
2a/B	8	3	3
D/B	0	0	0

The value of U+ is equal to the product of K_x and the horizontal head gradient at the boundary of the model. In using a value of 1 for U-/U+, it is assumed that the gradient upgradient and downgradient of the lake are the same, as well the hydraulic conductivities at those positions. Boring tests support the latter assumption, though contour maps of the groundwater table suggest that the gradient becomes slightly steeper further downgradient. However, the actual change associated with this value is difficult to observe due to the curvature of the head contours. Two values of U-/U+ have been used for runs where 2a/B = 2.

For the anisotropy, it is assumed that the aquifer is homogeneous. Hydraulic conductivity values are taken from the aquifer test (OpTech, 1996), which gives values of K_x=355 ft/day and K_z=118 ft/day, or a K_x/K_z of 3. Then the length from the boundary of the model to the lake edge is $L=2B(K_x/K_z)^{.5}$ or 3.46B.

As discussed in Section 4.1, recharge has the potential to create mounds of groundwater near surface water bodies, establishing local cells of flow. The recharge rate to the groundwater is 26 in/yr (Advanced Sciences, 1993). This gives a value of RL/U+B of 0.14.

There is no data available on the hydraulic conductivity of the pond sediment. Frequently, surface water bodies are lined with low conductivity bottom sediments that make the

vertical conductivity near the water body less than the vertical conductivity in the aquifer. However, due to lack of data, it is assumed that there is no such bottom resistance.

The values used for 2a, 600 and 1600 ft, have been discussed in Section 4.3.2. Data from boring tests suggest that the aquifer thickness is 200 ft, and it is assumed to be constant at 200 ft in the region near Snake Pond. This gives values for 2a/B of 2 and 8.

4.3.4 Results

Figures 4-3, 4-4, and 4-5 show results from the test. Water flows from the left to the right, and the bracketed area at the top is where the pond resides. The lines in the rectangle show contours of equal potential as well as streamlines. Looking at Figure 4-4 and 4-5, it is clear that for these scenarios nearly all water that flows under the pond and will eventually enter the pond. However, from figure 4-5, only the top half of the aquifer water will enter for regions where water travels only 400 ft under the pond. However, the bottom of the injection wells will be placed at -30 ft below mean sea level, which corresponds to 90 feet below the ground, or about half the thickness of the aquifer. From this it is concluded that all treated water injected upgradient of the pond will find its way into the pond.
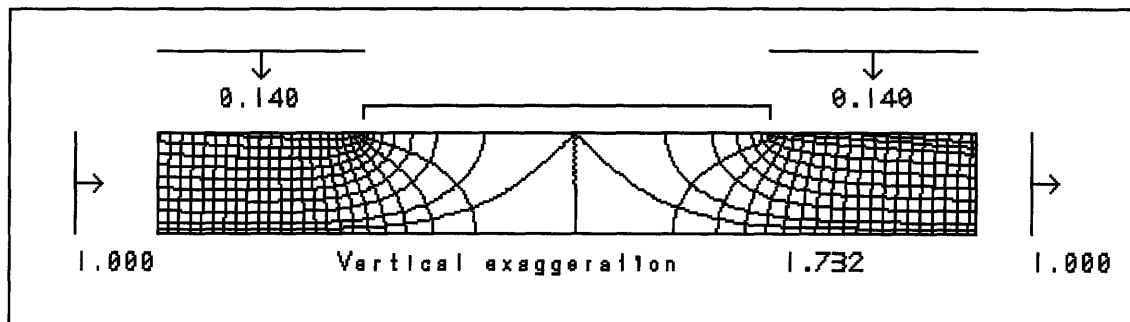
Figure 4-3: FlowThru Result for Run 1

28
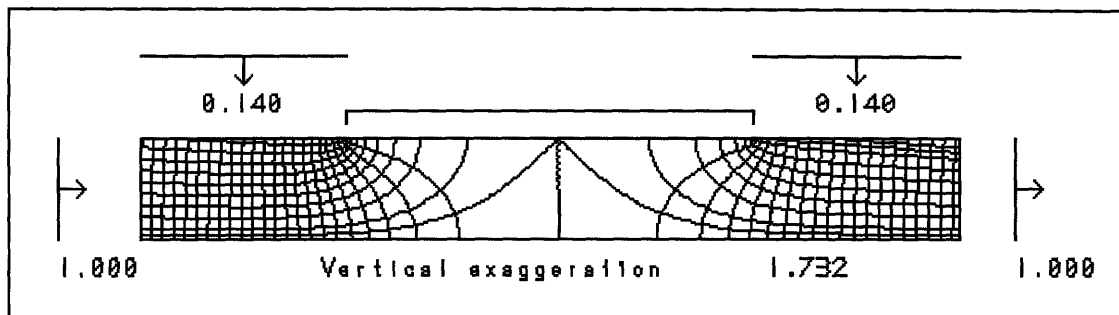
Figure 4-4: FlowThru Result for Run 2
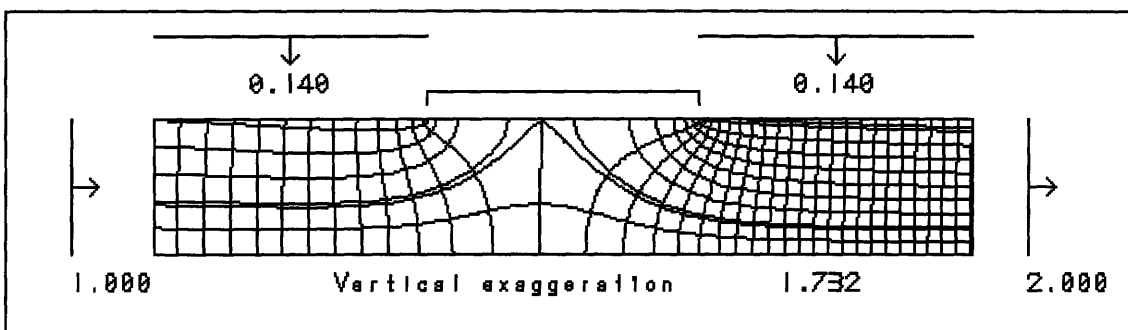
Figure 4-5: FlowThru Result for Run 3

4.3.5 Plan View Modeling

4.3.5.1 Assumptions

To estimate the flow of water entering Snake Pond, I have modeled the aquifer as a two-dimensional steady-state system in plan view, and assumed that the transmissivity of the aquifer remains constant. The aquifer injection test (Optech, 1996) shows maximum drawdown for a test well pumping at 500 gpm to be 6.8 ft. Since the aquifer is about 200 ft thick, the transmissivity drop should not be more than 5%, assuming a homogeneous aquifer. The model has assumed homogeneity, and this view is supported by boring tests from the preliminary study (Advanced Sciences, 1993).

The model does not take the dispersion of the treated water into the natural water into account. The longitudinal dispersion coefficient of the aquifer surrounding Snake Pond can be approximated by

$$D = \alpha \cdot v = \alpha \cdot \frac{k_x i}{\omega} \qquad \text{Eq. 4-2}$$

where

D =   Dispersion coefficient perpendicular to the flow

α =   Dispersivity of the aquifer

v =   Seepage velocity

k_x =   Hydraulic conductivity in the direction of flow

i =   Hydraulic gradient

ω =   Porosity

The longitudinal dispersivity is approximately equal to the median grain size of the aquifer (Hemond, 1994). Values for the hydraulic conductivity, the hydraulic gradient, and the porosity may be taken from the aquifer injection test. Grain sizes in the aquifer range from 0.454 to 1.04 mm, so letting α equal 0.614 mm, k_x equal 302 ft/day, ω equal 0.3, and i equal 5.3×10^{-4} ft/ft, the dispersion coefficient is approximately 1.0×10^{-3} ft²/day. The variance at the groundwater/surface water boundary will be approximately

$$\sigma^2 = 2Dt = 2D \frac{s}{k_x i \omega} \qquad \text{Eq. 4-3}$$

where s is the distance the water must travel from the reinjection well to Snake Pond. For the north and central reinjection wells, the distances are less than 250 ft, or a corresponding standard deviation of 10 ft, which is small enough to be negligible. At low velocities, molecular diffusion becomes the dominant dispersive mechanism, and transverse dispersion (Dy, Dz) is about equal to the longitudinal dispersion. And at high velocities, longitudinal dispersion is a much stronger process, so no significant in any direction is expected (Freeze and Cherry, 1979).

4.3.5.2 Derivation of Model Equations

The ground table elevation of the aquifer may be modeled using the law of superposition, if it is assumed that the differences in the water table elevations throughout the aquifer are negligible compared to the thickness of the aquifer, and that the system is in steady state. Then the head at any given point is the sum of the head caused by the naturally occurring field and that caused by each individual well. Assuming that the natural field is uniform, its effect on the head, h_{sat}, can be modeled as

$$h_{nat} = g_x x + g_y y + C \qquad \text{Eq. 4-4}$$

where

g_x =   Gradient in the x direction

g_y =   Gradient in the y direction

C   =   Head caused by field at the origin

The head due to a single well i, located at point (x_i, y_i), and pumping water out of the aquifer at a flow rate Q_i can be modeled using the Theim equation:

$$h(x, y) = \frac{Q_i}{4\pi T} \ln(\frac{r}{r_w}) \qquad \text{Eq. 4-5}$$

where r_w is the distance from the well for which $h(r_w)=0$, r is the distance from a point to the aquifer, or

$$r = \sqrt{(x - x_i)^2 + (y - y_i)^2} \qquad \text{Eq. 4-6}$$

and T is the transmissivity of the aquifer, defined as

$$T = \int K_x dz \qquad\qquad\qquad \text{Eq. 4-7}$$

where the integral is taken over the entire saturated zone. Adding equations 4-4 and 4-5 together gives the head a point (x, y):

$$h(x, y) = g_x x + g_y y + \sum_{i=1}^{n} \frac{Q_i}{4\pi T} \ln(\frac{r_i}{r_w}) \qquad\qquad \text{Eq. 4-8}$$

where n is the total number of wells.

4.3.5.3 Model Implementation

Plotting head contours, using equation 4-8, streamlines can be determined by drawing in lines orthogonal to lines of constant head. The use of equation 4-8 requires knowing the value of r_w. Lembke (1886 and 1887) gives one estimate for r_w as

$$r_w = b\sqrt{K/2N} \qquad\qquad\qquad \text{Eq. 4-9}$$

Where N is the natural recharge per year. For FS-12, equation 4-9 gives a value for r_w of 1000 ft. The values for head were calculated using a Visual Basic macro, the use of which is discussed in Appendix B. A plot of data, using well data from scenario 58 of the USGS model (Table 4-2) are given in figure 4-6, with a natural groundwater field heading directly south-southeast and a slope of 0.0005. The actual field tends to go south-southwest; however, Snake Pond tends to bring water towards it, since it has a much higher hydraulic conductivity than the ground.

4.3.5.4 Model Results

The drawdown predicted by this model does not agree completely with that predicted by the USGS model for areas far from the wells (see Figures 4-6 and 4-7). This is expected,

since the effects of Snake Pond were not accounted for in the model presented here. However, the region of interest is near the wells, for which the predictions of the two models are similar. Adding the effects of the naturally occuring field shows that the wells drawdowns are dominated by the regional groundwater table (see Figure 4-6), and since there are no areas for which the table slopes down from a injection well to an injection well, no injected water is expected to reenter the injection wells. The FlowThru model results (see Section 4.3.4) suggest that all reinjected water flowing under the lake will eventually flow into the lake. So at steady state, the amount of treated water entering the pond should be equal to the amount of water injected by wells whose paths lie along streamlines that the pond intercepts. Inspection of the USGS modeled groundwater table suggests that the water most likely to be intercepted by the pond is that from the northern and central reinjection wells, and the total flow due to these sources is 90,800 ft3/day. In comparison, Triantopolous (1996) calculated the flux of water entering Snake Pond to be 131,000 ft3/day. So up to 70% of the water entering Snake Pond may be from the reinjection wells. However, the injection wells may influence the flux of water entering Snake Pond, due to steeper hydraulic gradients near the pond. At the maximum, the water injected displaces none of the regional groundwater, and the total flow into Snake Pond is the 221,800 ft3/day. Then at the minimum, the portion of treated water in the Snake Pond inflow budget will be 40%.

Table 4-2: Well Positions and Pumping Rates, Scenario 58

| North Axial Extraction Wells				North Injection Wells			
Well ID	Easting (ft)	Northing (ft)	Pump Rate (gpm)	Well ID	Easting (ft)	Northing (ft)	Pump Rate (gpm)
EW10	868590	252820	19.6	IRW5	867839	252086	-50.48
EW11	868630	252660	19.6	IRW6	867931	251990	-50.48
EW12	868630	252520	19.6	**Central Injection Wells**			
EW13	868600	252400	27.1	Well ID	Easting (ft)	Northing (ft)	Pump Rate (gpm)
West Axial Extraction Wells				IRW7	868023	251810	-52.05
Well ID	Easting (ft)	Northing (ft)	Pump Rate (gpm)	IRW8	868092	251566	-62.75
EW6	868071	252332	32.1	IRW9	868018	251399	-72.75
EW7	868225	252305	32.1	IRW10	868129	251150	-82.75
EW8	868346	252300	37.1	IRW13	868520	250640	-52.75
EW9	868470	252260	37.1	IRW14	868560	250383	-49.05
South Axial Extraction Wells				**South Injection Wells**			
Well ID	Easting (ft)	Northing (ft)	Pump Rate (gpm)	Well ID	Easting (ft)	Northing (ft)	Pump Rate (gpm)
EW14	868570	252200	22.1	IRW15	868718	250349	-25.86
EW15	868538	252054	22.1	IRW16	868920	250317	-26.36
EW16	868546	251933	22.1	IRW17	869112	250273	-26.86
EW17	868620	251789	22.1	IRW18	869136	250350	-29.26
EW18	868810	251680	22.1	IRW20	869263	250538	-29.26
EW19	868921	251390	27.1	IRW21	869365	250571	-29.26
EW20	868779	250494	22.1	IRW22	869466	250605	-29.27
EW21	868842	250536	22.1	IRW23	869549	250638	-35.36
EW22	868950	250580	22.1	IRW24	869669	250672	-35.36
EW23	869050	250640	22.1	IRW25	869770	250705	-37.36
EW24	869189	250702	17.1	IRW26	869872	250739	-38.36
EW25	869331	250757	22.1	IRW27	869973	250772	-43.51
EW26	869443	250826	17.1	IRW28	870150	250840	-36.51
EW28	869591	250899	51.7	IRW29	870170	251070	-39.51
EW30	869736	250979	51.7	IRW30	870169	251149	-38.51
EW32	869879	251080	56.7				
EW34	870087	251209	76.7	**Sandwich Municipal Well #5**			
EW35	869989	249878	47.1	Well ID	Easting (ft)	Northing (ft)	Pump Rate (gpm)
EW36	870106	249851	47.1	SW5	866400	248450	135.01
EW37	870275	249910	47.1				
EW38	870346	250021	47.1				
EW39	870376	250145	47.1				
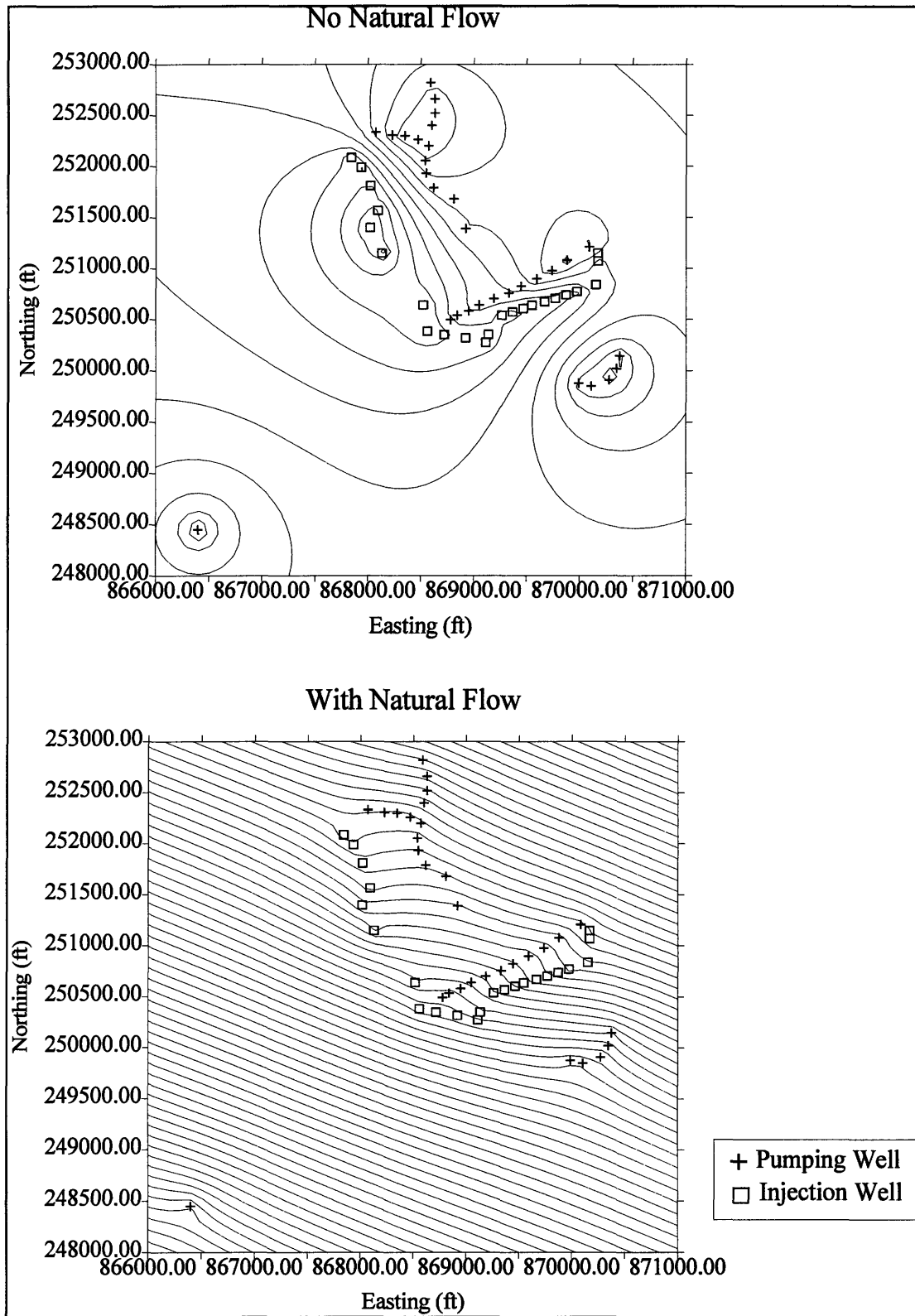
Figure 4-6: Comparison of Head Potentials with and without Natural Flow
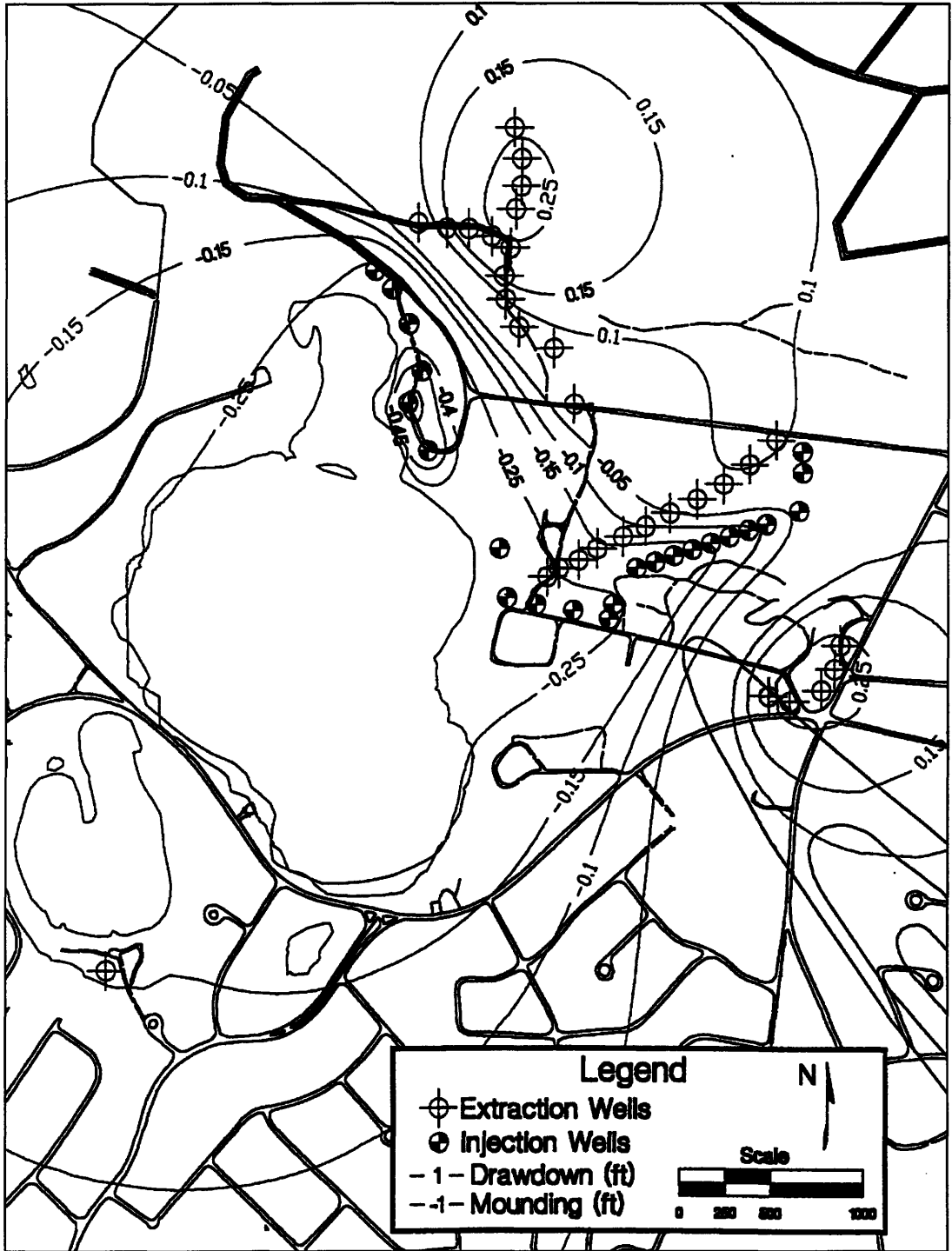
Figure 4-7: USGS Predictions for Mounding and Drawdown

5. Mixing Characteristics of Snake Pond

5.1 Introduction to the Snake Pond Thermal Model

To date, very little physical data has been collected for Snake Pond. Jacobs Engineering measured Snake Pond's temperature profile in the summer of 1996 (Jacobs Engineering, Nov. 1996), and found uniform temperatures throughout, with slightly warmer water along the bottom of the pond. Similarly, a baseline water quality study (Department of Environmental Quality, 1984) revealed no sign of stratification on August 12, 1980. However, no other data on the thermal nature of Snake Pond could be found.

To study the mixing mechanisms occurring in Snake Pond, I have developed a Snake Pond Thermal Model (SPTM), based on a model by Ryan and Harleman (1971). The model considers the pond as a finite stack of horizontal layers, each of uniform temperature. The layers gain or lose thermal energy via direct absorption of solar radiation, molecular diffusion of heat from neighboring elements, longwave radiation from the water to the air and vice versa, evaporation, conduction, and mixing due to unstable temperature gradients (i.e., temperature decreasing with elevation,) or due to wind.

5.2 Assumptions with Caveats

This model is one dimensional—the temperature is a function of depth, and has no horizontal dependence. In reality, ponds have horizontal profiles, due to wind tilting the epilimnion, heterogeneity in the flux of energy, irregular bottoms, and inflows and outflows of water. However, the lack of large water fluxes through Snake Pond, as well as the lack of observed stratification support the use of a one-dimensional model.

The sides and bottom of the pond are assumed to be insulated. In the model, energy flows into the pond only through the surface, and any energy from solar radiation reaching the bottom or sides stays entirely within the lake. The movement of water through the ground is

slow enough that the conduction of heat will be on the order of molecular diffusion, i.e., $2.04 \times 10^{-9} m^2/sec$, which is negligible compared to the transport of heat into and out of the surface. There is also energy associated with cold groundwater entering, and warm water exiting. The USGS, in modeling the FS-12 area, has calculated that about 60,000 ft^3 of water enter Snake Pond each day. Assuming that groundwater is 10°C and the pond water is 25°C, there are 2.6 x 10^7 kcals per day lost to groundwater flow. In comparison, on a very cloudy day in the middle of January, the SPTM model calculates that the sun will radiate 1150 kcal/m^2/day. Multiplied by the surface area of the lake, this gives 3.8 x 10^8 kcals per day, or 15 times the energy lost to groundwater. The energy of groundwater flow may be more significant if energy flows are not evenly distributed over the lake. Therefore, some error may accompany this assumption.

Via similar arguments, ground water flows into and out of the pond, but the thermal consequences associated with such flows are assumed to be negligible. In ponds with large inflows, temperature differences between entering water and pond water induce effects such as entrainment and the rising or falling of inflowing water due to differences in water density. Large inflows also cause advection and turbulence. Snake Pond has a low flow and a large flux area, making these terms insignificant.

Solar radiation energy is assumed to be uniform over the surface. A non-uniform radiation field may heat the sides of the lake, and therefore the horizontal layers, unevenly. The effect is more pronounced on lakes having steep bottom slopes, as does Snake Pond along the southern side. However, non-uniformity affects warming of the sides, and therefore has greater impact on the layers closer to the surface. Wind mixing will distribute the energy evenly, so the effects of a non-uniform field would be insignificant on the epilimnion, but potentially significant on the hypolimnion. In the case of Snake Pond, no thermocline or possibly a very deep thermocline is expected, so a non-uniform radiation field will most likely have the same effect as a uniform one.

The SPTM works only for bodies of fresh water. The presence of salt in lakes affects the densities of water, which in turn changes the convective mixing and the strength of stratification for a given temperature profile. Data from DEQE suggest insignificant salt concentrations in Snake Pond.

The SPTM does not accurately predict temperatures when ice has formed on the surface. When a lake freezes, evaporation and conduction processes change significantly, and the ice reflects back a larger portion of incoming solar radiation. The model does not account for these effects. Since a lake's temperature profile at any given time depends on the profile's history, it may seem that initial conditions must be set for a time when there is nothing frozen. However, the model's lack of accuracy during periods of freezing should not significantly affect its predictive power during the rest of the year. When there is no mixing between the surface layer and the layers below, as happens when the surface is ice, and the interaction between them is limited to molecular diffusion, the rate of temperature change of the surface layer is almost entirely a function of the current weather conditions. Without mixing, the mass of water which is affected by atmospheric conditions is reduced to a thin layer near the surface, while the area through which energy can be exchanged remains the same. Temperatures move to equilibrium more rapidly, so that, as long as there is not a very sudden change in weather conditions, the time at which all the ice on the surface changes into water depends almost entirely on the weather conditions of that time, and does not depend strongly on the temperature of the surface or the temperature profile of the lake. While the model cannot predict the behavior of a lake with a surface of ice, it can predict the behavior of a lake with a surface of water, even if the water is at 0°C; therefore, it should be able to determine the time at which the surface changes from ice to water. Moreover, the water in a lake tends to stay near 4.1°C when covered with ice, so that, as long as the model's temperatures below the surface are close to 4.1°C, it should still be able to predict the temperatures of a lake after a period of freezing, even without new initial conditions.

5.3 Formulas and Algorithms Employed

The SPTM is a finite element model, which calculates the energy flux entering and exiting each layer as well as the turbulent mixing processes that cause entrainment.

SPTM takes into account the flow of energy via five different routes (Figure 5-1): direct solar radiation (of which a quantity ϕ_S is absorbed directly at the surface, and a quantity $\phi(y)$, is absorbed throughout the pond), molecular diffusion, evaporation (ϕ_e), conduction (ϕ_c) ,
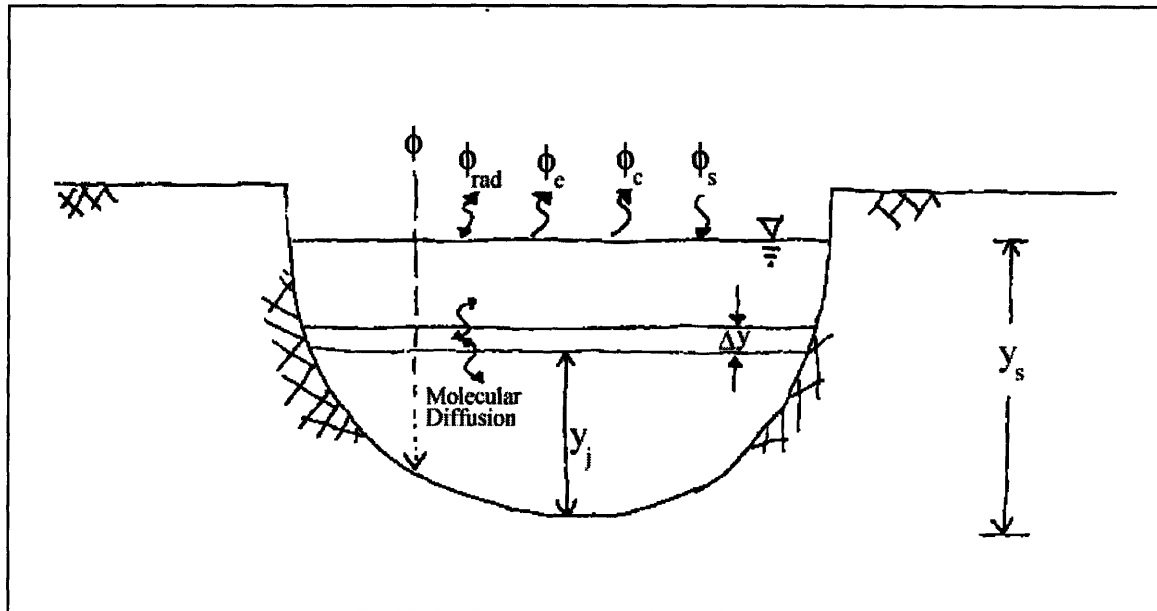
39

Figure 5-1: Flow of Energy in the SPTM

and the net longwave radiation emitted by air and water (ϕ_r),. The model also accounts for mixing due to unstable temperature gradients and to wind .

5.3.1 Direct Solar Radiation

Solar radiation can be converted to heat energy directly in the fluid or along the bottom or sides. A significant amount will be converted directly at the surface of the pond. The transmission of heat at the surface is given by

$$\phi_s = \phi_o \beta \qquad\qquad \textbf{Eq. 5-1}$$

where

ϕ_S = radiation absorbed at the surface (energy/area/time)

ϕ_O = net incident solar radiation

β = fraction of incident radiation absorbed at the surface

The change of the surface layer temperature, due to this radiation, will be

$$\Delta T_{solar} = \frac{1}{\rho C_w A_1 \Delta y}(\phi_s A_{surf})\Delta t$$

Eq. 5-2

where

ρ	=	Density of water
C_w	=	Heat capacity of water
A_1	=	Average area of the surface layer
A_{surf} =		Area of the surface of the pond

The SPTM uses an empirical relationship developed by Baker (1979) to determine the net incident solar radiation as a function of latitude, cloud cover, and time of year. The function is shown in section A.1. The values are subject 10-15% error, due to haze and atmospheric refraction.

The value for β has been measured to be between 0.4 and 0.5 (Ryan and Harleman, 1971). The SPTM model uses $\beta = 0.45$. Therefore, 45% of the radiation is absorbed at the surface, and the remaining solar radiation will travel through the water, the transmission decreasing exponentially with depth:

$$\phi(y) = \phi_o(1-\beta)e^{-\eta(y_s-y)}$$

Eq. 5-3

where

ϕ = Radiation transmitted at elevation y

η = Extinction coefficient (length^{-1})

y_S = Depth of the pond (see Figure 5-1)

y_j = Elevation from bottom of pond

The extinction coefficient varies from lake to lake, and is further discussed in Section 5.4.2.

By conservation of energy, the energy absorbed by a layer j will be the difference of the energy entering from the top of the layer, minus the energy leaving the bottom. Therefore, the temperature change in layer j due to direct solar radiation will be

$$\Delta T_{solar} = \frac{1}{\rho C_w A_j \Delta y_{sur}} (\phi_{ju} A_{ju} - \phi_{jb} A_{jb}) \Delta t$$

Eq. 5-4

where

A_j = Average area of layer j

A_{ju} = Area of the upper bound of layer j

A_{jb} = Area of the lower bound of layer j

The SPTM assumes that the area varies linearly with the depth of the layer, so that

$$A_j = \frac{A_{ju} + A_{jb}}{2}$$

Eq. 5-5

5.3.2 Molecular Diffusion

Heat will travel via molecular diffusion if there are gradients in temperature. The temperature change associated with diffusion in time Δt is:

$$\Delta T_{diff} = \frac{\alpha}{A_j \Delta y} [\frac{(T_{j+1} - T_j)}{\Delta y} A_{ju} - \frac{(T_j - T_{j-1})}{\Delta y} A_{jb}] \Delta t$$

Eq. 5-6

where α = the molecular diffusion coefficient = 2.04 x 10^{-9} m^2/sec.

5.3.3 Longwave Radiation

All objects containing heat emit longwave radiation. Net radiation flux within the water body is assumed to be negligible, but the radiation exchange between water surface and air has been taken into account. For the SPTM, water is assumed to radiate like a black body (i.e., proportional to T^4), while the radiation of air is based on a semi-empirical formula by Swinbank (1971). Assuming a 3% reflection of the longwave atmospheric radiation by the water surface,

$$\phi_{rad} = \phi_w + \phi_a = 0.97[kT_{ws}^4 - 0.937 \times 10^{-5} kT_a^6 (1.0 + 0.17c^2)]$$

Eq. 5-7

where

ϕ_{rad} = Net longwave radiation out of pond

ϕ_w = Longwave radiation emitted by water

ϕ_a = Longwave radiation emitted by atmosphere

k = Boltzmann constant (1.171×10^{-6} kcal/m^2/°K^4/day)

T_{ws} = Temperature at the water surface (°K)

T_a = Air temperature, 2 meters above the surface (°K)

c = Fraction of sky covered by clouds

and the net temperature change in the surface layer due to longwave radiation is

$$\Delta T_{rad} = \frac{-1}{\rho C_w A_{surf} \Delta y_{sur}} (\phi_{rad} A_{ysur}) \Delta t \qquad \text{Eq. 5-8}$$

Note that temperatures are in degrees Kelvin and that the temperatures are being raised to high powers. For even small differences in water and air temperatures, this term will cause large ΔT, which can overshoot equilibrium temperatures and become unstable if the time elements are not small enough. Due to this instability, the SPTM uses a small Δt of a quarter day (6 hours).

5.3.4 Evaporation and Conduction

Evaporation may be expressed in terms of vapor pressures, via Dalton's law of mass transfer, modified to allow for wind:

$$E_m = \rho(a + bW)(e_s - \psi e_a) \qquad \text{Eq. 5-9}$$

where

E_m = Mass flux

a,b = Empirical constants

W = Wind speed, 10m above the surface

e_s = Saturation vapor pressure at the surface water temperature

e_a = Saturation vapor pressure at air temperature

ψ = Relative humidity

The energy associated with evaporation is

$$\phi_e = E_m(L_v + c_w T_s)$$
Eq. 5-10

where

L_v = Latent heat of vaporization

T_s = Surface water temperature in degrees C

c_w = Heat capacity of water

Conduction losses are usually related to a temperature gradient with respect to saturation vapor pressure. This is called the Bower ratio:

$$\phi_c = N \frac{T_s - T_a}{e_s - \psi e_a}$$
Eq. 5-11

where N is an empirical constant. Rohwer (1931) has developed a field equation to calculate the evaporation and conduction losses:

$$\phi_c + \phi_e = (0.000308 + 0.000185W)\rho(e_s + \psi e_a)(L + cT_s + \frac{T_s - T_a}{e_s - \psi e_a})$$
Eq. 5-12

with

ρ in kg/m^3,

W in m/sec,

e_s, e_a in mm Hg,

ψ as a fraction,

L_v in kcal/kg,

c in kcal/kg/$^\circ$C

and the net temperature change of the surface layer due to evaporation and conduction is

$$\Delta T_{e\&c} = \frac{-1}{\rho C_w A_{surf} \Delta y_{sur}} [(\phi_e + \phi_c) A_{ysur}] \Delta t$$

Eq. 5-13

5.3.5 Convective Mixing

Convection is the transport of heat due to the movement of fluid. In this case, convective mixing refers to mixing due to warm, light water rising, and cold, heavy water sinking. The buoyancy fluxes cause turbulence within the layers, and mixing occurs. To account for convective mixing, any neighboring layers with a positive $d\rho/dy$ are allowed to fully mix until their temperatures, and thus their densities, are the same. It is assumed that no energy is lost in this procedure, so that when two layers mix,

$$T_{new} = \frac{T_n V_n + T_m V_m}{V_n + V_m}$$

Eq. 5-14

where n and m are the layers that will mix. Appendix A contains a more detailed account of how the model handles convective mixing.

5.3.6 Wind Mixing

As air moves across a body of water, it imparts momentum to the surface, inducing currents and turbulence which can penetrate a significant depth into the water. To account for wind mixing, the SPTM contains a wind mixing routine (wind mixer) which calculates the

energy imparted by wind to the lake, and mixes the lake until the potential energy gained from mixing is equal to the kinetic energy gained from the wind, minus dissipation effects. The wind mixing algorithm employed by the SPTM is based on the one developed by Bloss and Harleman (1977). Their report contains detailed explanations of all the formulas presented here, unless another source is noted.

The rate of kinetic energy transmitted from wind to the surface of the lake is

$$\frac{1}{A_s}\frac{d(KE)}{dt} = \tau u_s = \rho u_*^2 u_s \qquad\qquad \text{Eq. 5-15}$$

where

KE = Kinetic Energy

τ = Shear stress applied to surface

u_s = Drift velocity of the surface

ρ = Density of water at the surface

u_*^2 = Drift velocity $(=\sqrt{\tau/\rho}\,)$

Equation 5-15 cannot be used directly, because τ and u_s are not parameters that are measured easily. There has been extensive research into developing relationships between these data and other more measurable parameters, particularly to the wind speeds at a given height above the lake. Assuming that all the momentum that enters the surface of the water is transformed into kinetic energy, and that the wind speed at a given height is directly proportional to the drift velocity, it can be shown that

$$\tau = C_z \rho_a W_z^2 \qquad\qquad \text{Eq. 5-16}$$

where

C_z = Friction coefficient (dimensionless) for a given height above the surface, z

ρ_a = Density of air

W_z = wind speed at height z

Coantic (1978) has found an empirical relationship of $C_{10}=(1+0.05W_{10})\times10^{-3}$, which has been employed in the model. However, the value is subject to considerable error. The effects of stratification in the air will influence its accuracy, and the value changes considerably when the water is less than 2.5m deep (Hicks, 1972).

For the drift velocity, Bloss and Harleman (1977) assumed that $u_s=u_*$, based on qualitative arguments. This is only an order of magnitude approximation, but experiments on the relationship between the drift velocity and the shear velocity in lakes are few. For lack of a better value, the SPTM also uses this assumption.

The final form of the equation relating kinetic energy to wind speed is

$$KE = \frac{(C_z \rho_a W_{10}^2)^{3/2}}{\rho^{1/2}}$$

<div align="right">Eq. 5-17</div>

When a layer from the hypolimnion becomes entrained in the epilimnion, heavy water moves up, and cold water moves down. Since the center of gravity of the lake is moved up, potential energy increases:

$$dPE = A_s \Delta \rho g (y_s - y) dy / 2$$

<div align="right">Eq. 5-18</div>

where $\Delta \rho$ is the density difference between the upper and lower layer and g is gravity.

The kinetic energy from the wind will be converted to potential energy via entrainment of the hypolimnion into the epilimnion. However, dissipation prevents all the energy from being converted. When the wind is mixing a weakly stratified region, much of the kinetic energy is

converted to turbulent kinetic energy. This energy remains in layers that have already been mixed. If the stratification is very strong, energy is dissipated due to internal wave energy and turbulent energy cascades. Ryan and Harleman developed the following semi-empirical equation for the ratio of potential energy gained to kinetic energy lost:

$$f(Ri) = \frac{\Delta PE}{\Delta KE} = 0.057 Ri\{\frac{29.5 - \sqrt{Ri}}{14.2 + Ri}\}$$

Eq. 5-19

where Ri is the Richardson number, defined as

$$Ri = \frac{g\Delta\rho l}{\rho\sigma^2}$$

Eq. 5-20

where l is the turbulent length scale, and σ is the turbulent velocity scale. Assuming that the length scale is the depth to which wind mixes, and that the velocity scale is the shear velocity, we can write

$$Ri = \frac{g\Delta\rho h}{\rho u_*^2}$$

Eq. 5-21

The SPTM takes the temperatures calculated by the convective mixer, calculates the energy imparted to the lake by wind, and mixes the pond from the surface down, so that

$$KE = \int_{y_z}^{y_s} \frac{dPE(y')/dy'}{f(Ri(y'))} dy'$$

Eq. 5-22

where y_z is the elevation above which wind mixing occurs. The mixer does this by mixing layer by layer, starting from the top, until all the kinetic energy is spent. The appendix contains more information on the routine the SPTM uses for wind mixing.

5.3.7 Ice on the pond

Ice on the surface of the pond will tend to insulate the water below, so that it does not freeze all the way to the bottom. When ice has formed on the surface of the pond, the SPTM calculates all energy fluxes as before and mixes the pond to account for convection, but it assumes that there are no mixing effects from the wind. Preventing the icy surface from mixing with layers below is enough to keep the model accurate for times following a freeze, as discussed in Section 5.2.

5.4 Model Inputs

The SPTM model requires six inputs: Bathymetry, extinction coefficient, air temperature, relative humidity, cloud cover, and wind speed. This section discusses how data were obtained for the SPTM. The appendix contains more technical information on how these data are entered into the model.

The model also requires that an initial condition be input. For all the model runs performed, the initial condition was a uniform profile of 4.1°C, on December 31st, 1992.

5.4.1 Bathymetry

SPTM requires knowing the area of each discretized element. For Snake Pond, these areas were determined using a map produced by the DEQE (1984) (Figure 5-2). The map shows four contours; however, four elements are not sufficient for modeling. Some interpolation was used to get 10 contour lines (9 elements).
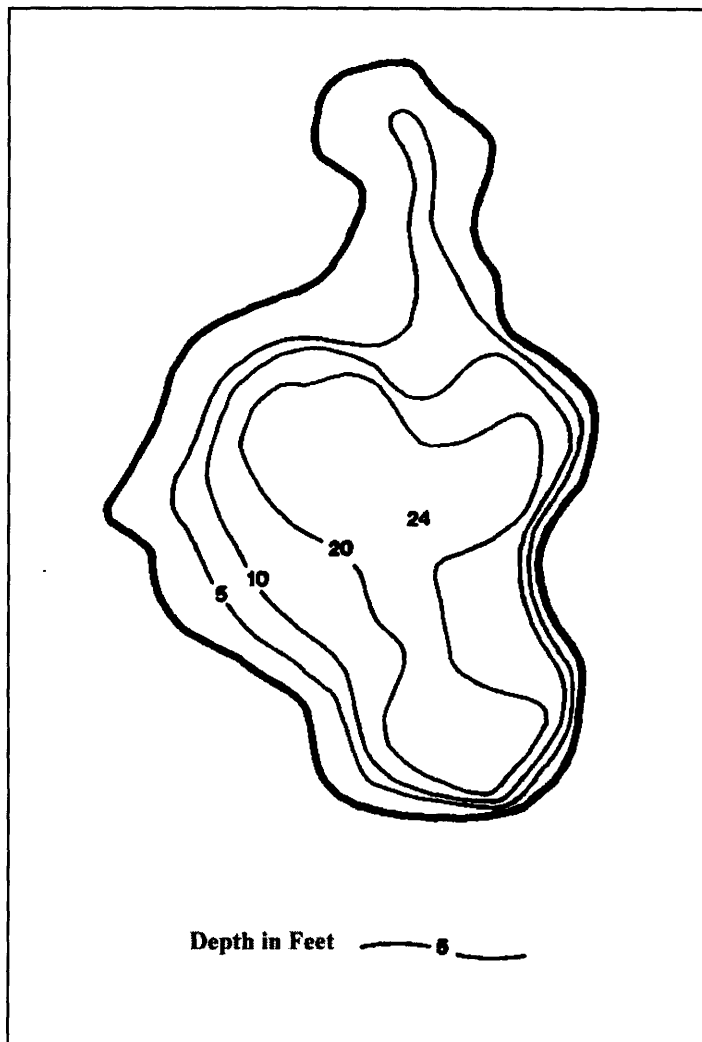
Figure 5-2: Contour Map of Snake Pond

5.4.2 Extinction Coefficient

The extinction coefficient is a measure of the water's ability to absorb and scatter radiation (see Eq. 5-3). Its value depends on the concentration of particulates in the water, such as suspended solids, organic detritus, and phytoplankton—the concentrations of which vary from lake to lake. The extinction coefficient for a given body of water can change over time, due to seasonal changes in organic input or an increase in phytoplankton. Also, the value is a function

of the frequency of light, with yellow-orange light being absorbed less than other colors. These factors contribute to inaccuracies in extinction coefficient measurement. One rough method of determining the extinction coefficient is to lower a highly visible target into the water, and measure the depth at which the target is no longer visible. A standardized target is the Secchi disk, and numerous relationships have been developed between the Secchi depth and the extinction coefficient. Sverdrup et al. (1942) have developed an empirical relationship:

$$\eta = 1.8 / z_s \qquad\qquad\qquad \textbf{Eq. 5-23}$$

where z_s is the Secchi depth. Duerring and Rojko (1984) have measured z_s=2.4m at Snake Pond, which gives an extinction coefficient of 0.75 m^{-1}. There is considerable scatter in the extinction coefficient/secchi depth relationship, and extinction coefficients can vary throughout a body of water. However, at the time of this study, more useful data for determining the extinction coefficient was not available for Snake Pond. Section 5.7.2 discusses the sensitivity of the lake to changes in this coefficient.

5.4.3 Meteorlogical Data

Meteorlogical data was obtained from web page of the National Oceanic and Atmospheric Administration (NOAA). The data downloaded was for 1993 and contains the average wind speed, dew point temperature, high and low temperatures, and cloud cover for each day. These data were taken from Logan Airport in Boston, Massachusetts. Some calculation was needed to turn these data into a form usable by the model. Air temperatures for the model were assumed to be constant throughout the day, equal to the average of the high and low temperatures. No differentiation was made between day and night values for any weather data. The vapor pressure was determined using a formula by TVA (1972):

$$\psi e_a = \exp[2.3026(\frac{7.5 T_d - 236.9}{T_d + 395.5} + 0.6609)]$$

Eq. 5-24

where T_d is the dew point temperature in degrees Farenheit, and e_a is in millimeters mercury. The appendix contains more information on the conversion of the weather data for the model.

5.5 Modeling Procedure

The SPTM was written on an Excel Spreadsheet and a Visual Basic macro. The macro calculates the effects of conductive wind mixing, while the spreadsheet calculates energy flow into and out of the pond, plus the effects of molecular diffusion. For each time t, the model does three sets of calculations. The first calculation is based on energy flows without mixing. The second calculation takes the results of the first, and changes them to account for convective mixing. The third takes the results of the second, and changes them to account for wind mixing. After all calculations are made, the model moves on to time $t+\Delta t$, and the cycle repeats.

The temperatures calculated in the first set are a function of the day's weather parameters and the temperatures of the water during time t-Δt. This formula for a non-surface layer j is

$$T_{jt} = T_{j(t-\Delta t)} + \Delta T_{j(solar)} + \Delta T_{j(diff)}$$

Eq. 5-25

and for the surface layer,

$$T_{1t} = T_{1(t-\Delta t)} + \Delta T_{1(solar)} + \Delta T_{1(diff)} + \Delta T_{rad} + \Delta T_{e\&c}$$

Eq. 5-26

where all ΔT's have been defined in Section 5.3. Note that ΔT_{diff} is related to the amount of heat diffusing from both the upper and lower boundaries of the layer. But the temperature of the

lowest layer diffuses only at its upper boundary, since the lake is assumed to have an insulated bottom. And the temperature of the top layer diffuses only through its lower boundary, since the diffusion of heat to the air is accounted for in $\Delta T_{e\&c}$.

After the energy flows have been calculated, wind and conductive mixing effects are calculated in the manners described in Sections 5.3.5 and 5.3.6.

For a more detailed account of the SPTM program and its formulas, the reader is directed to appendix A.

5.6 Model Test

Since the data available for Snake Pond are less than adequate for determining the model's ability to predict temperatures, this model has been tested using data from Gull Pond, a larger kettle pond in Cape Cod, with a depth of 60 ft, which has been studied extensively. The data for Gull Pond is from the DEQE, who collected light and temperature data during 1993.

As with Snake Pond, running this model for Gull Pond required meteorological and bathymetrical data. The meteorological data used was the same as that for Snake Pond, taken from 1993. As for bathymetry, the areas for each layer of Gull Pond were calculated from a contour map (Figure 5-3).

The model also requires an extinction coefficient for Gull Pond. In the 1993 study, a Secchi number of 5.7m was obtained. Using equation 5-23, this suggests an extinction coefficient of about 0.3138 m^{-1}. However, as is detailed in Section 5.7.2, the use of this value in the model predicts a deeper thermocline than was actually measured. A more accurate coefficient was calculated from light data obtained in the same study. This data was derived by using two light meters, one just above the water, and one at some depth. The amount of light at both places was measured simultaneously. From Equation 5-3, we can write

$$\ln(\frac{\phi(y)}{\phi_o}) = \ln(1-\beta) - \eta(y_s - y) \qquad \text{Eq. 5-27}$$

The light data for Gull Pond are shown in Figure 5-4. A linear regression was performed to determine the value for η. Data points near the surface are erratic, due to wave motion, so values above 4 m were not included in the linear regression analysis. Based on the regression, the average extinction coefficient for toes days at Gull Pond is 0.449 m^{-1}, with a standard deviation of .012 m^{-1}.

The model was run using the inputs described above, and with an initial temperature of 4.1°C throughout the pond on December 31st, 1992. Comparing the calculated results to the actual temperatures recorded, the model is found to be a good predictor of the actual temperature profile, as shown in Figure 5-5. There is some discrepancy in the eplimnion temperatures—this may be attributed to the fact that weather conditions used in the model do not account for diurnal fluctuations. However, the formation of the thermocline and the temperature of the hypolimnion are less sensitive to short time fluctuations, and are more accurately predicted by the model. This test suggests that the model predictions for Snake Pond may be reasonably reliable.

5.7 Model Results

This section contains the results of the model runs for Snake Pond, using weather data from 1993. Some caution should be exercised when interpreting the results of this model. The stratification behavior that the SPTM predicts is based on daily averages, and does not account for the fluctuation of weather conditions from day to night. Weather conditions for other years will significantly alter many of results presented here. And the extinction coefficient can vary over time.

5.7.1 Results for Snake Pond, 1993

The SPTM was run for Snake Pond, using weather data from 1993. Temperature profiles for a few selected days are shown in Figure 5-6. For the most part, there appears to be no significant stratification, which is consistent with the findings of the DEQE (1984) and Jacobs
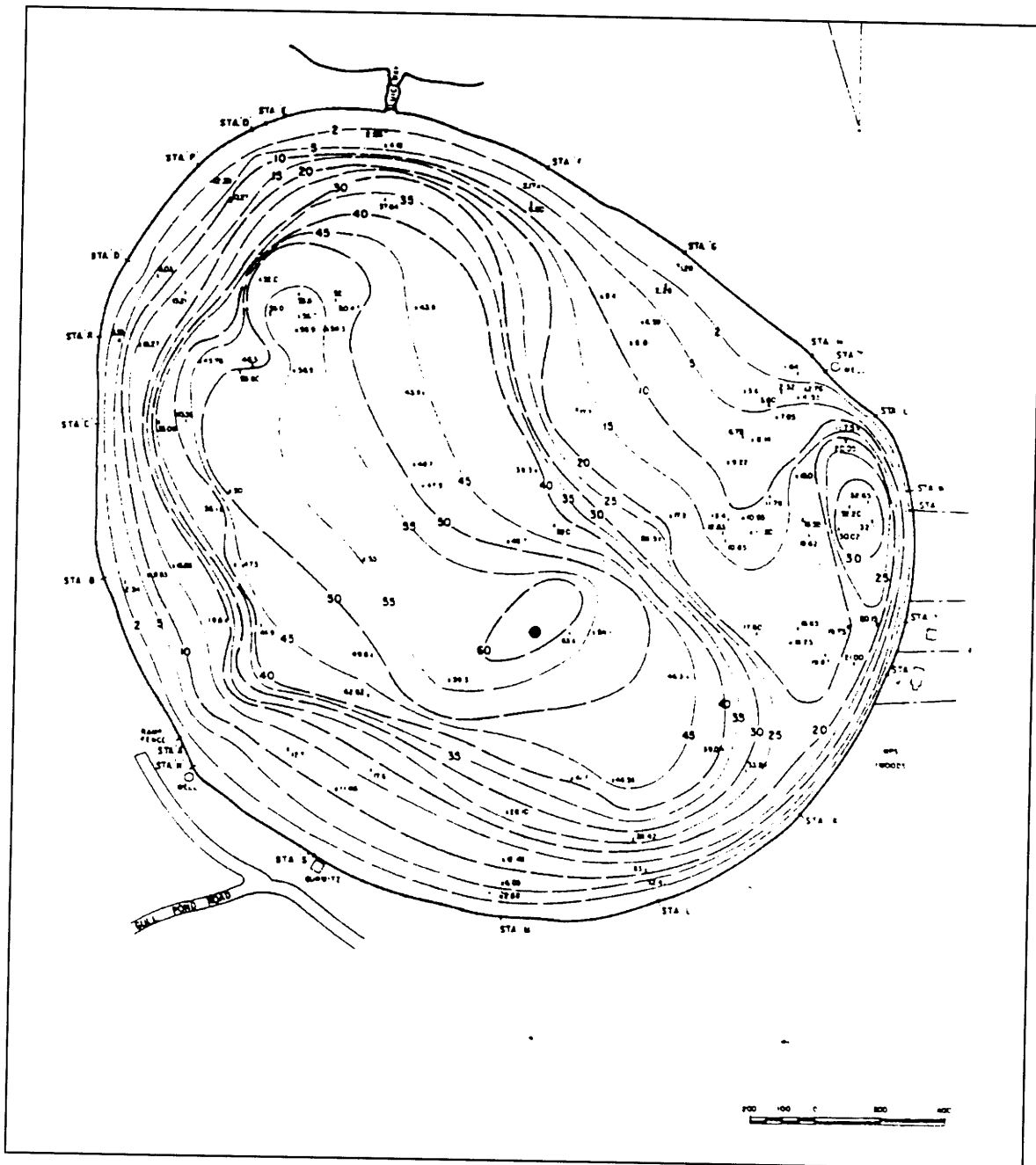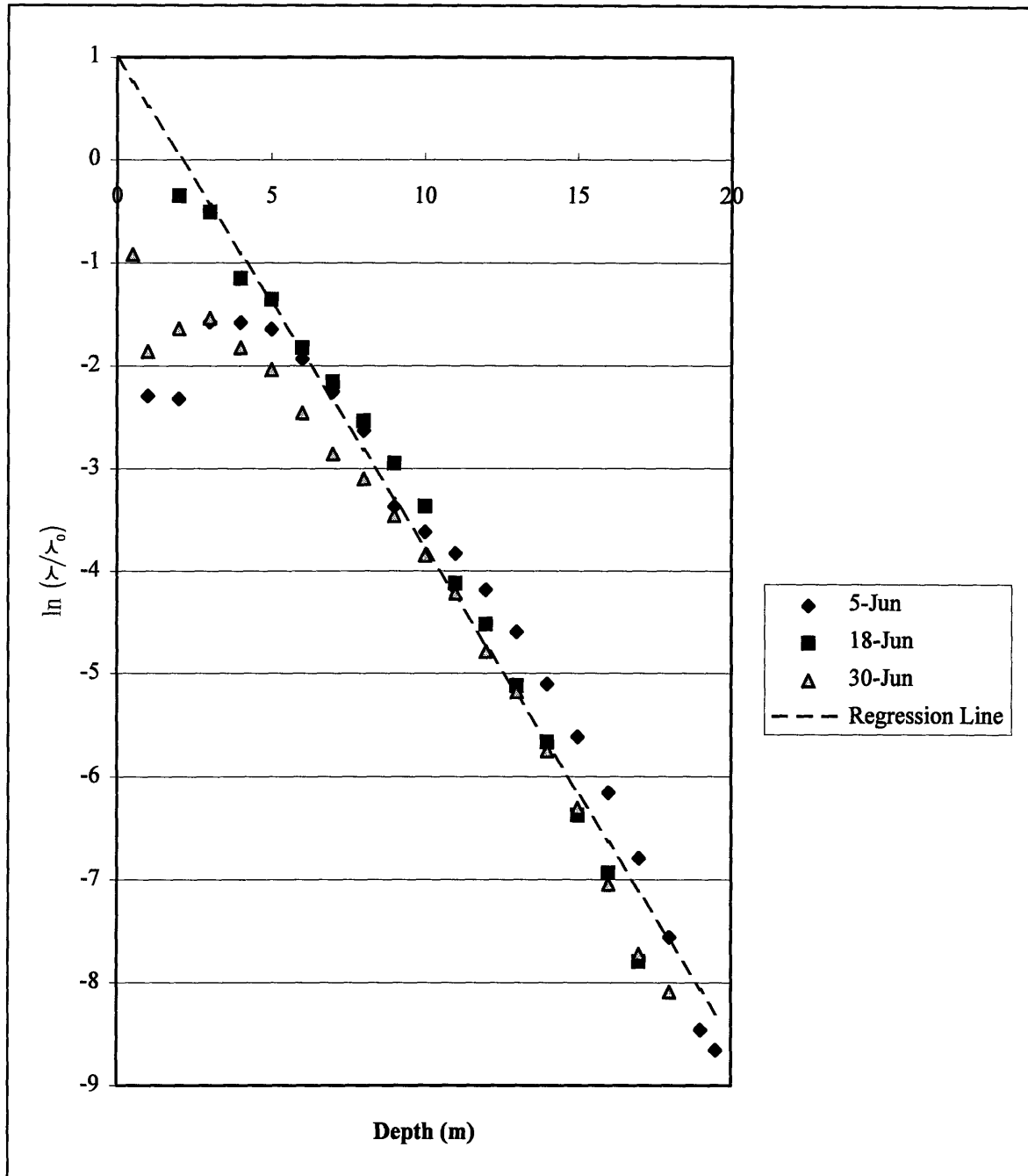
55

Figure 5-3: Contour Map of Gull Pond

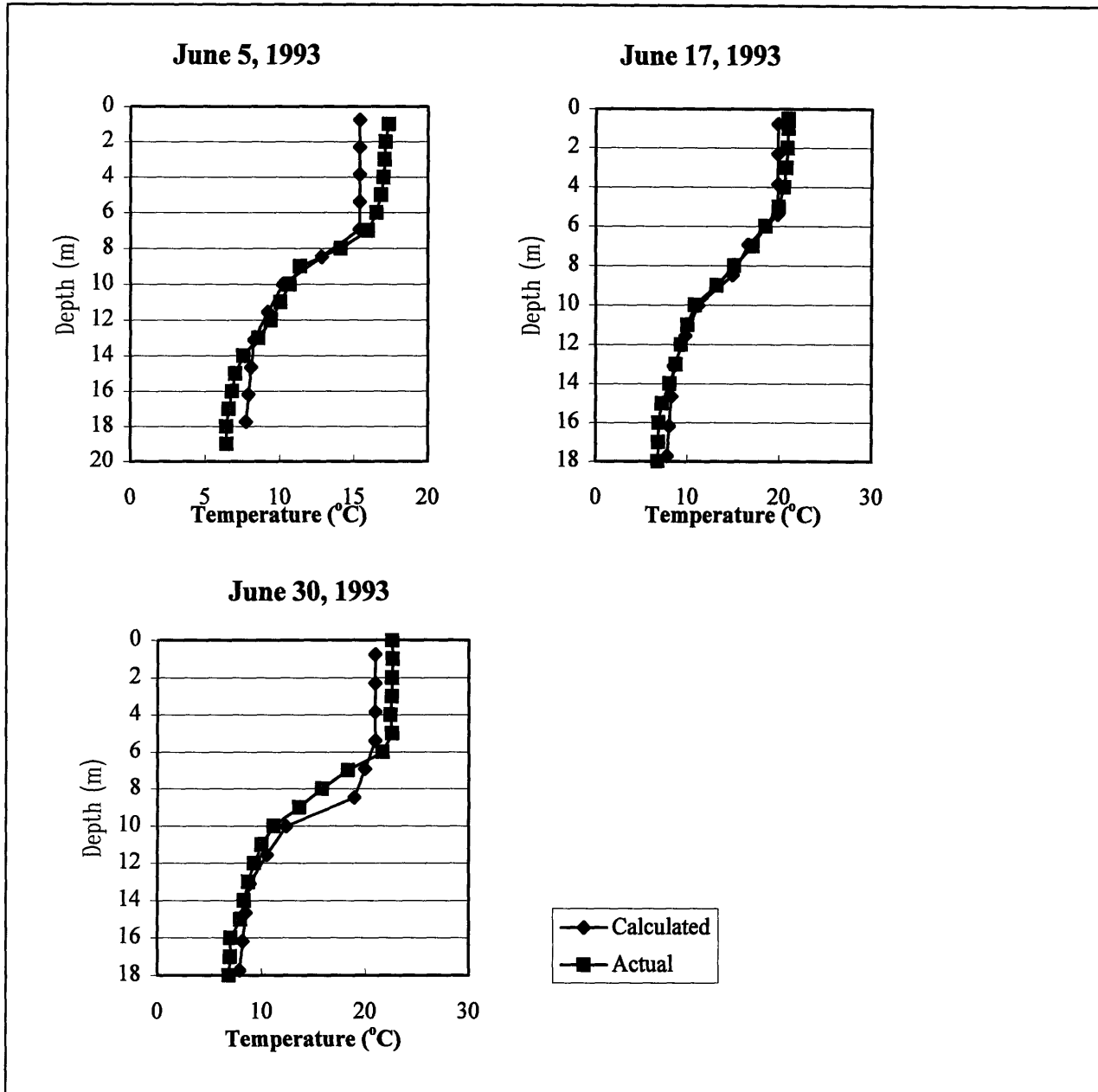**Figure 5-4: Plot to Determine the Extinction Coefficient of Gull Pond**

Figure 5-5: Model Test for Gull Pond

Engineering (1996). Included in Figure 5-6 is the temperature profile for August 3 (Julian day 215), which is the day in 1993 during which the SPTM predicts the largest difference between the temperature of the surface and the temperature of the bottom of the pond. This stratification lasts about eight days, with a maximum ΔT_{sb} of 4.7°C, where ΔT_{sb} is defined as the difference between the temperature of the surface and bottom of the pond. ΔT_{sb} can be used as a rough measure of the degree of stratification, though a small value of ΔT_{sb} may be the result of a

temperature profile with a very sharp dT/dy over a short depth, while a large ΔT_{sb} may represent a profile with a gradual dT/dy over a longer depth.

Figure 5-7 shows a plot of both the surface and bottom temperatures as functions of time. Within 1993, the model predicts that the temperature of the surface and bottom are exactly the same 300 out of 365 days in the year. Figure 5-8 shows values of ΔT_{sb} versus the duration for which the value is held over the course of 1993, and shows that ΔT_{sb} is rarely above 3°C. Figure 5-9 shows that long stratification events are rare, and that the pond rarely has a positive ΔT_{sb} for longer than four days.
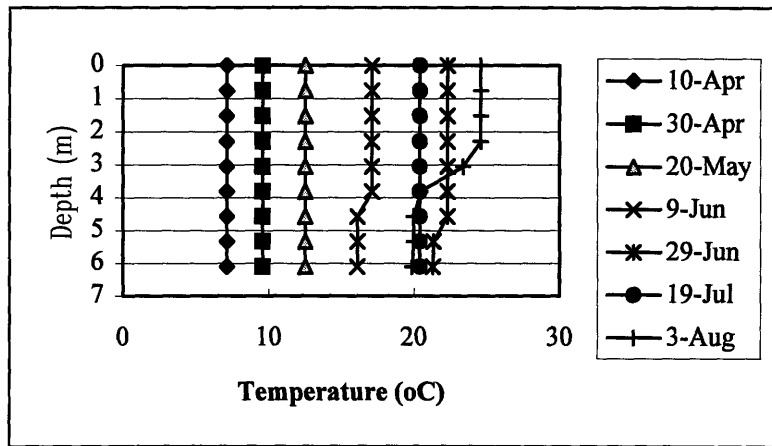

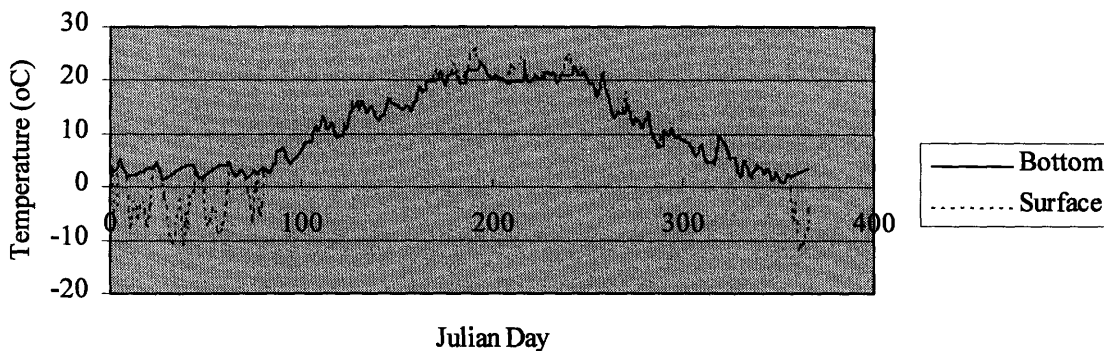**Figure 5-6: Temperature Predictions by the SPTM for Snake Pond, 1993**

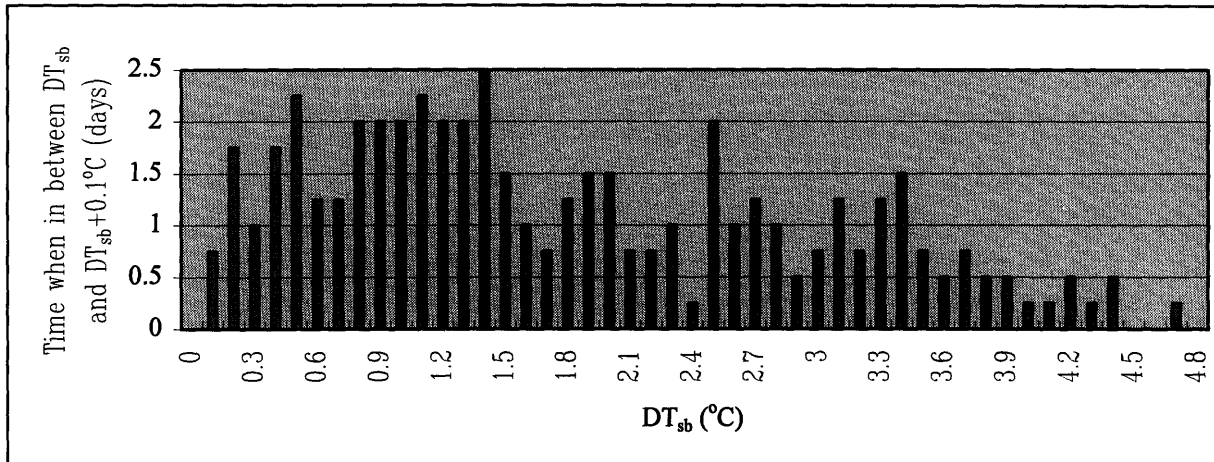**Figure 5-7: Variation of Surface and Bottom Temperatures with Time**

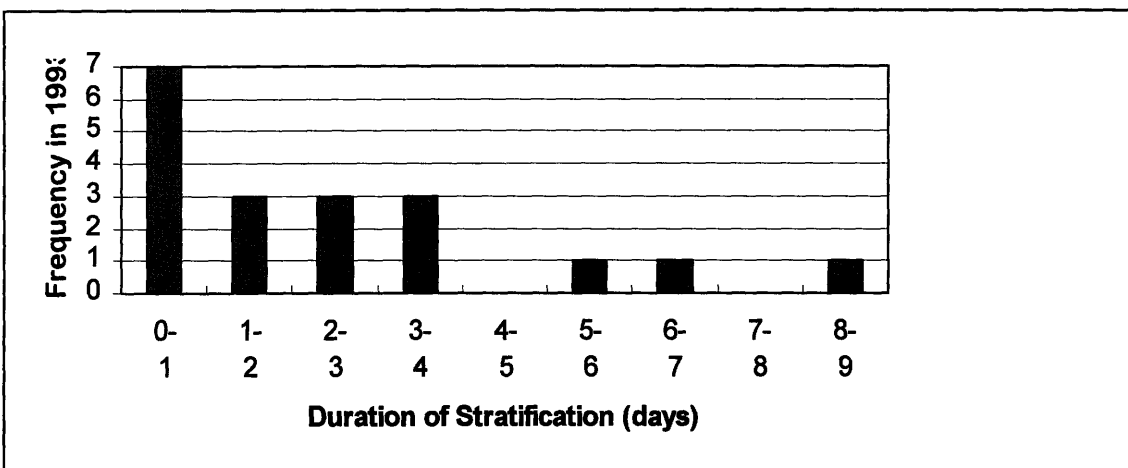**Figure 5-8: Durations for ΔT_{sb} values**

Figure 5-9: Frequency of Stratification Durations

5.7.2 Sensitivity Analysis

Originally, Gull Pond was tested using an extinction coefficient based on the Secchi depth. The value for this extinction coefficient is about ¾ the value obtained using light meter data. The results of this test are shown in Figure 5-10. The great change in temperature profile prompted a look into the sensitivity of Snake Pond's calculated profiles to its extinction coefficient. Figure 5-11 shows values for the maximum duration for which ΔT_{sb} is positive, given various extinction coefficients. The stepwise movement of the maximum duration is due

60
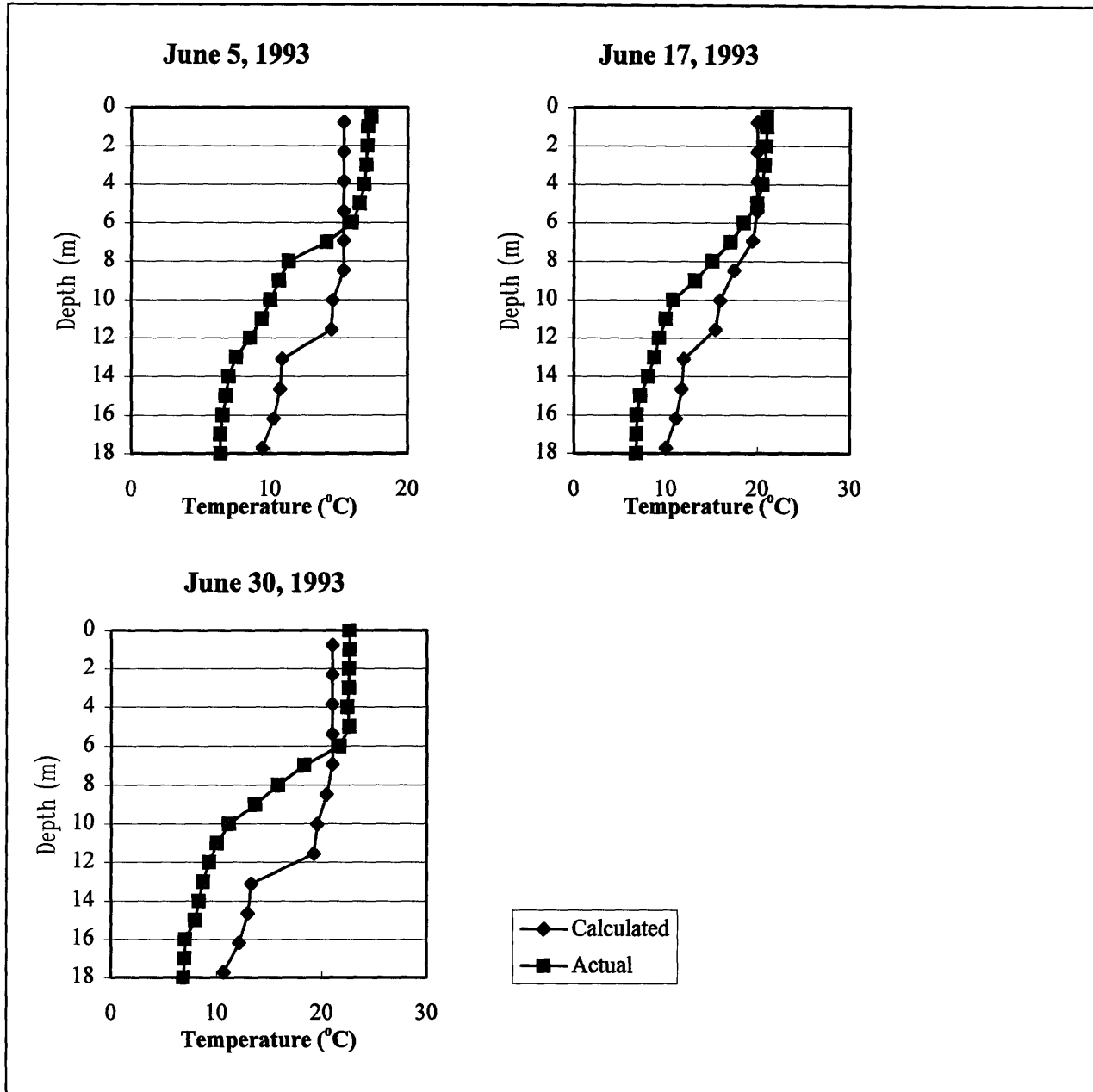
Figure 5-10: Gull Pond Results, Using Secchi Depth as Basis for Extinction Coefficient

to blocks of stratification periods growing and merging together. For 1993 data, it would appear that the extinction value measured (0.75 m^{-1}) can vary from 0.4 to 1.5 with little change in the stratification durations. However, this measure will depend on weather conditions, since the stepwise movement makes for sudden changes in the maximum duration. For extinction
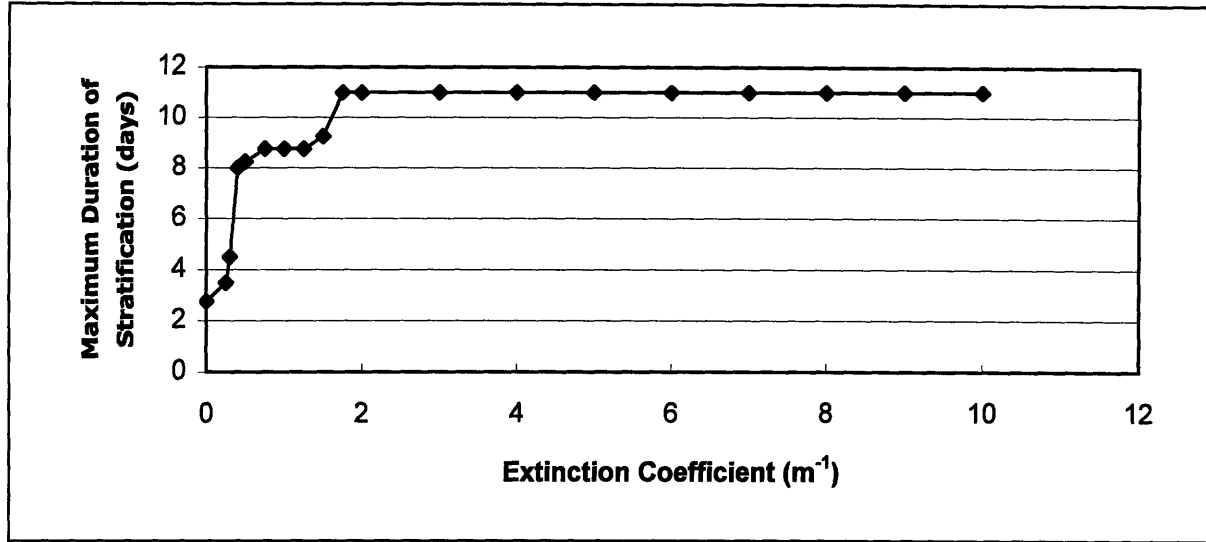
Figure 5-11: Sensitivity of Stratification of Snake Pond to the Extinction Coefficient

coefficients between 0 to 10 m^{-1}, the maximum durations are between 2.75 and 11 days. So it would appear that the stratification of the pond is not very sensitive to the extinction coefficient.

5.7.3 Wind Mixing Analysis

Figure 5-12 shows a series of graphs for Gull Pond, comparing results from a normal model run and a run with no wind mixing. Figure 5-13 shows the same comparison for Snake Pond. Whereas wind mixing only slightly affects the temperature profile of Gull Pond, there is a pronounced stratification in Snake Pond if the wind mixing effects are ignored. The difference between the behaviors of Gull and Snake ponds to wind mixing may be attributed to two variables: greater extinction coefficients and a more shallow bottom in Snake Pond. The first parameter causes a greater amount of heat to be absorbed close to the surface of Snake Pond, which in turn causes a greater degree of stratification. The second parameter allows means that there is less water to for wind to mix. The potential energy associated with mixing a layer increases with depth. Even with Gull pond, we see that the wind induced turbulence can penetrate up to 8 m, which is deeper than Snake Pond.
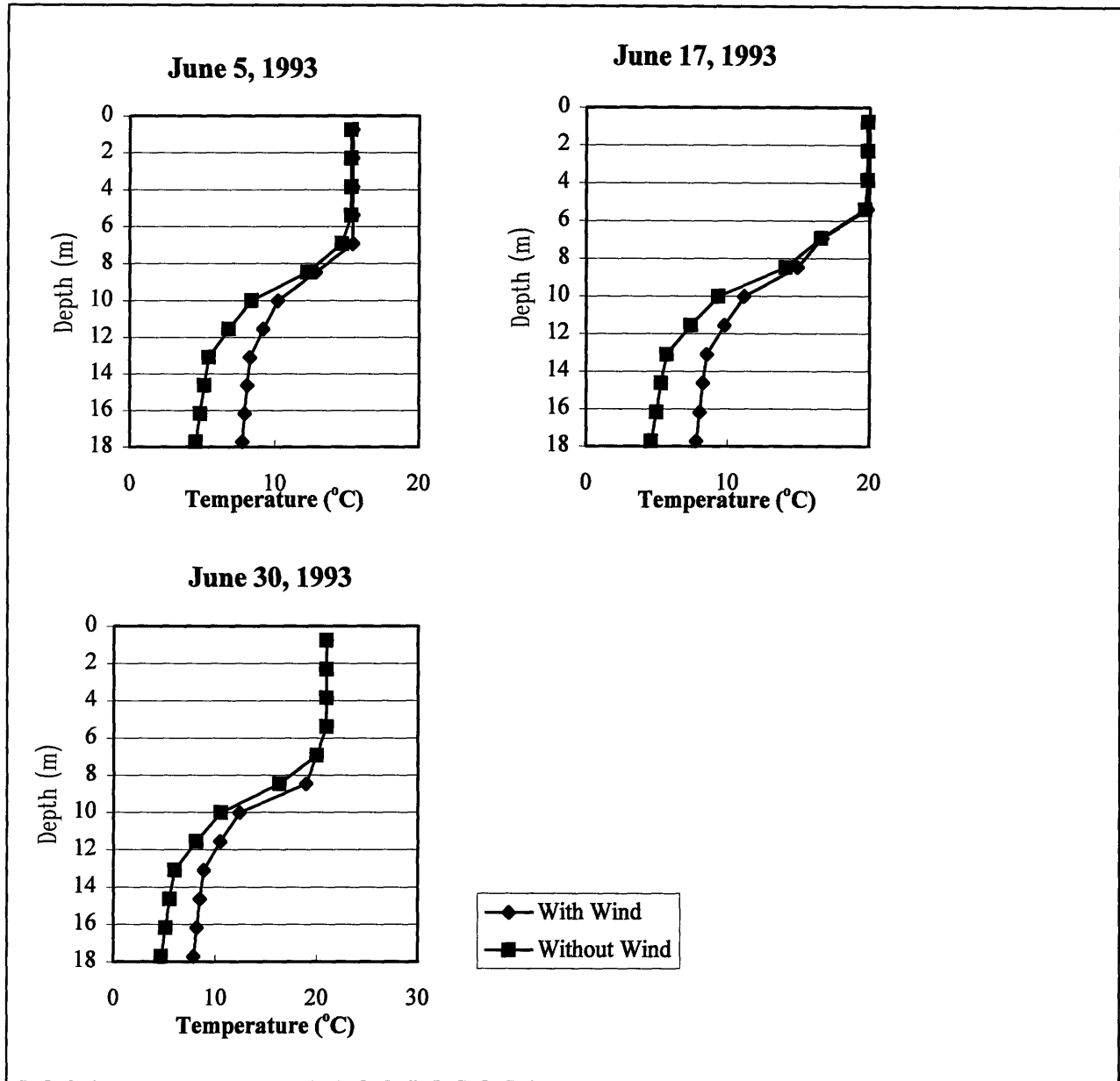
Figure 5-12: Wind Mixing Analysis for Gull Pond
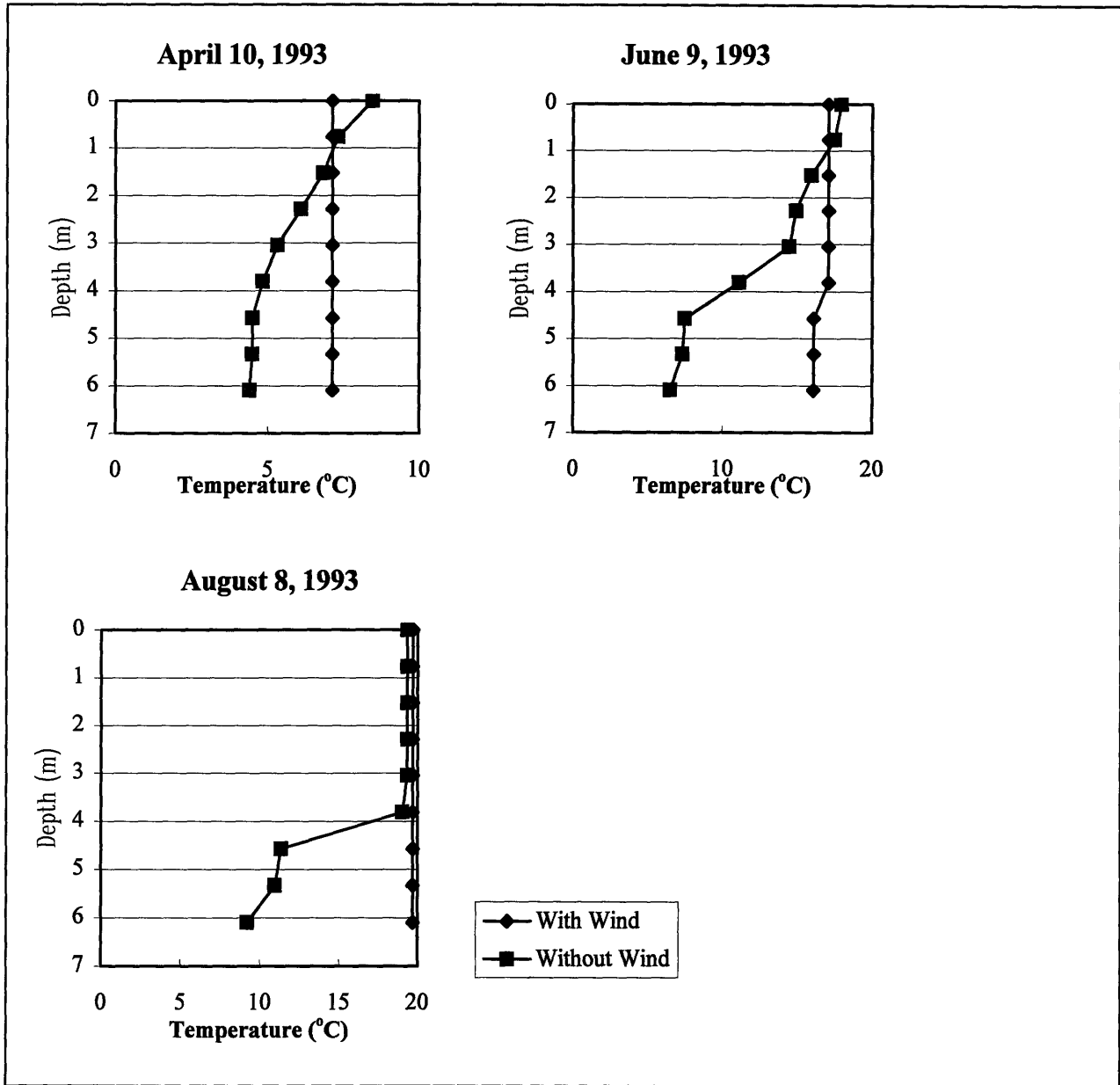
Figure 5-13: Wind Mixing Analysis for Snake Pond

5.8 Summary and Conclusions

To understand the mixing mechanisms within the pond, a model was created which predicts the temperature profile of the pond. This model can also be used to analyze the sensitivity of the pond to a number of variables. The model predicts temperature changes based on energy fluxes and mixing mechanisms. A test of the model, using data from Gull Pond,

shows that it is a good predictor of the thermal stratification for small freshwater ponds with no significant surface inflow or outflow.

The model predicts that there will be no significant stratification in Snake Pond, and that the pond will fully mix for most of the year. However, there may be temporary stratification which should be considered when examining the transport of chemicals through the pond. As a conservative limit, an analyst studying the pond should check the effects of a stratification event lasting at least 11 days.

The mixing of Snake Pond is greatly wind driven. Without the presence of wind, the model predicts significant stratification in the pond. Since wind mixing is much more important than convective mixing, the nature of the turbulence in Snake Pond will be the type associated with wind-driven turbulence, with a turbulent length scale at any point equal to depth of the pond.

While the extinction coefficient used in the model was not very precise, the model calculates that the temperature profile of Snake Pond is insensitive to changes in the extinction coefficient, due to the strong influence of wind mixing. Any change in the quantity of suspended solids caused by the pump and treat system should not significantly affect its mixing characteristics.

6. Summary and Conclusions

In order to better understand the movement of water into and inside Snake Pond, a number of models were implemented. Two groundwater models were used together to predict the flow of injected water into Snake Pond. Using FlowThru, it was determined that mounding did not cause a significant effect on the flow of water, and that the length of the pond permitted all injected water upgradient to enter the pond. This result was insensitive to changes in recharges or changes in pond lengths.

A model was developed to observe the water table in plan view. While not as sophisticated as the USGS or Jacobs models, it is a reasonable predictor of the water table heads near the wells. From this model, it was determined that the natural water field dominates the water table contours, and that little to no water from the injection wells will cycle back to the pumping wells.

Combining results, it was determined that all water injected upgradient of the pond will travel into the pond. All of the north and central injection wells appear to be upgradient, and the portion of groundwater entering Snake Pond that will be treated water is between 40% and 70%, which is consistent with results from the USGS and Jacobs models. However, it is expected that the reinjection wells will displace much of the natural groundwater, and the actual portion should be closer to 70%.

To determine mixing mechanisms occurring in Snake Pond, a thermal model was created which accounted for energy fluxes, and wind and convective mixing. Applying the model to Snake Pond, there appears to be no significant stratification, and the pond can be considered a mixed tank year-round. Goddard (1997) has predicted that the injection wells will cause a decrease in dissolved organic carbon, which may lower the extinction coefficient. However, the model shows that the thermal structure of Snake Pond is insensitive to changes in the extinction coefficient. The model also predicts that wind is the dominant mixing mechanism, and that the bottom of the pond is mixed by wind very frequently, with 11 days being the maximum duration

for which the pond does not fully mix, using 1993 weather data. The lack of stratification allows even calm winds to effectively mix the pond.

The thermal structure has been modeled adequately, and while the surface water/groundwater interaction is not fully understood, work by Goddard (1997) suggests that the quality of the water in Snake Pond is insensitive to the quantity of treated water entering. So the quantity calculated in this report is sufficient to predict the impacts of the ETR to Snake Pond.

Bibliography

Advanced Sciences, Inc., Remedial Investigation/Feasibility Study: FS-12 Study Area:
Draft Report. December, 1993.

Advanced Sciences, Inc. Remedial Investigation Report: FS-12 Study Area, Final Copy. Cape
Cod: January, 1995.

Automated Services Group, Inc., Risk Assessment Handbook, Massachusetts Military
Reservation, Cape Cod, Massachusetts. Cape Cod, September 1994.

Baker, Clarance, Solar Radiation Availability on the Surface of the United States as Affected by
Season, Orientation, Latitude, Altitude and Cloudiness. Arno Press: New York, 1979.

Bloss, S. And Harleman, D., Effect of Wind-Mixing on the Thermocline Formation in Lakes and
Reservoirs. MIT Department of Civil Engineering, Parsons Laboratory for Water
Resources and Hydrodynamics Report No. 249: Cambridge, November 1979.

Bosch, Christophe, J. Gagnon, et al., An Assessment of Water Supply Issues and Current and
Alternative Remedial Schemes for Fuel Contaminated Groundwater, Including a Case
Study: Fuel Spill 12 at the Massachusetts Military Reservation. Department of Civil
and Environmental Engineering Massachusetts Institute of Technology. May 20,
1996.

Cherkauer, Douglas, and Zager, John, "Groundwater Interaction with a Kettle-Hole Lake:
Relation of Observations to Digital Simulations." Journal of Hydrology, v.109, 1989.

Coantic, M., "Coupled Energy Transfer and Transformation Mechanisms Across the Ocean-
Atmosphere Interface", Proceedings of the 6th International Heat Transfer Conference,
Vol. 6, Toronto, Canada, 1978.

Freeze, R. A., and Cherry, J. A., Groundwater. Prentice Hall: Englewood Cliffs, NJ, 1979.

Goddard, Scott, Chemical Impacts to a Cape Cod Pond due to the Reinjection of Carbon-Treated
Groundwater. MIT Department of Civil and Environmental Engineering:
Cambridge, 1997.

Hemond, Harold, and Fechner, Elizabeth, Chemical Fate and Transport in the Environment.
Academic Press: Boston, 1994.

Hicks, B.B. "Some Evlauations of Drag and Bulk Transport Coefficients Over Water Bodies of

Different Sizes", Boundary Layer Meteorology, Vol. 3, 1972.

Jacobs Engineering, Plume Containment System, Groundwater Modeling Results: Draft Report. Cape Cod: July, 1996.

Knoll, M.D., et al., "Characterization of a Sand and Gravel Aquifer Using Ground-Penetrating Radar, Cape Cod, Massachusetts." U.S. Geological Survey Toxic Substances Hydrology Program: Proceedings of the Technical Meeting, Monterey, California, March 11-15, 1991; edited by Mallard, G.E., and Aronson, D.A.; U.S. Geological Survey Water-Resources Investigations Report 91-4034.

Lembke, K.F. "Groundwater Flow and the Theory of Water Collectors". The Engineer, J. Of the Ministry of Communications: 1887.

Lerman, Imboden, and Gat, ed., Physics and Chemistry of Lakes, 2nd Ed. Springer-Verlag: New York, 1995.

Massachusetts Military Reservation, "Environmental Cleanup: An Overview," Fact Sheet 96-6. Cape Cod: April, 1996.

Massachusetts Military Reservation, "Fuel Spill 12 Ground-Water Plume," Fact Sheet 96-12. Cape Cod: December, 1996.

Masterson, John P. And Paul M. Barlow, "Effects of Simulated Groundwater Pumping and Recharge on Groundwater Flow in Cape Cod, Martha's Vineyard, and Nantucket Island Basins, Massachusetts. U.S. Geological Survey, Open-File Report 94-316, 1994.

McBride, M.S., and Pfannkuch, H.O., "The Distribution of Seepage within Lakebeds". Journal of Research, United States Geological Survey, v.3: Sept 1975.

Munk, W.H. and Anderson, E.R., "Notes on a Theory of the Thermocline", J. Marine Research 7, 1948.

Nield, Simon, and Townley, Lloyd, "A Framework for Quantitative Analysis of Surface Water - Groundwater Interaction: Flow Geometry in a Vertical Section". Water Resources, June/July 1994.

Optech Co., Plume Containment Design: Fuel Spill-12 Injection Test Technical Memorandum. v.1: October 1996.

Rohwer, C., "Evaporation from Free Water Surfaces", U.S. Department of Agriculture, Technical Bulletin No. 271, December 1931.

Rollbein, Seth, The Enemy Within. Association for the Preservation of Cape Cod, 1995.

Ryan P., and Harleman, D., Prediction of the Annual Cycle of Temperature Changes in a Stratified Lake or Reservoir: Mathematical Model and User's Manual. MIT Department of Civil Engineering, Parsons Laboratory for Water Resources and Hydrodynamics Report No. 137: Cambridge, Massachusetts, April 1971.

Sverdrup, H.U., et al., The Oceans. Prentice-Hall: Englewood Cliffs, NJ, 1942.

Swinbank, W. C., "Long-Wave Radiation from Clear Skies", Quarterly Journal of the Royal Meteorological Society of London, Vol. 89, July 1963.

Tennessee Valley Authority, "Fontana Reservoir 1966 Field Data, Part I, Temperature and Flow Data", Report No. 17-91, TVA, Division of Water Control Planning, Engineering Laboratory: Norris, Tennessee, March 1969.

Townley, Lloyd, Barr, A.D., and Nield, S.P., FlowThru: An Interactive Program for Calculating Groundwater Flow Regimes Near Shallow Surface Water Bodies. CSIRO Division of Water Resources Technical Memorandum, Version 1.1: January 1992.

Townley, Lloyd, Wetlands of the Swan Coastal Plain: Interaction Between Lakes, Wetlands and Unconfined Aquifers. v.3. Water Authority of Western Australia: 1994.

Triantopoulos, Dimitris, Modeling of a Jet Fuel Spill in the Groundwater at the Massachusetts Military Reservation. MIT Department of Civil and Environmental Engineering, Cambridge: 1996.

Winter, T.C., "Numerical Simulation of Steady-State Three Dimensioal Groundwater Flow Near Lakes". Water Resources Res 14:255-254.

Appendix A: The Snake Pond Thermal Model Program

The Snake Pond Thermal Model (SPTM) is composed of one spreadsheet and one Visual Basic macro, both written in Excel version 7.0a. The two parts work together to calculate the temperature profile. The spreadsheet initially contains all meteorological and bathymetrical data, as well as formulas for calculating temperatures of each layer, *sans* mixing. Each quarter day's temperature is a function of that quarter day's weather as well as the water temperatures of the previous quarter day. The macro, going in quarter day increments, reads water temperatures and calculates the effects of mixing on the temperature profile. A new profile, for which wind effects have been accounted, is returned to the spreadsheet, overwriting the original temperatures. The depth of wind energy penetration is also calculated and put into the spreadsheet. The macro then asks the spreadsheet to calculate the temperatures for the next quarter day, and the cycle is repeated. While the entire model could be written as a macro, separating the model into two parts keeps the program simpler. The long, repetitive calculations are more easily handled on the spreadsheet, and the macro has only been employed where logic decisions are necessary.

The input sheet is the same as the output sheet, and the macro destroys all the spreadsheet formulas that calculate unmixed temperatures. To run the model again, a copy of the original data must be pasted onto the SPTM spreadsheet. For more information on how to use Microsoft Excel and Visual Basic, the reader is referred to user guides published by Microsoft (1994).

A.1 Excel Spreadsheet Format and Formulas

The SPTM spreadsheet is used as both the input and output file. It contains all input data necessary, as well as formulas which calculate temperature changes due to the flux of energy through the pond, and the diffusion of heat within the pond. These formulas do not account for convective and wind mixing. This task has been assigned to the Visual Basic macro (next

71

section). Originally the model was run using $\Delta t = 1$ day, but due to instabilities associated with the longwave radiation term, this was brought down to $\Delta t = 6$ hours, using constant weather conditions for four consecutive Δt's.

The input sheet is the same as the output sheet, and the macro destroys all the spreadsheet formulas that calculate unmixed temperatures. To run the model again, a copy of the original data must be pasted back into the SPTM spreadsheet.

Column A: Marks quarter days (Row 6 is quarter day 1, Row 1469 is quarter day 1464 (end of day 366)).

Column C to K: Layers of the pond (Row C is the bottom layer, Row K is the surface layer). See below for formulas.

Column L: Serves two purposes: From Row 1 to Row 4, shows data for the area and elevation of the surface. From Row 6 to Row 1469, the macro outputs the depth of wind mixing penetration.

Column N: Air Pressure (mm Hg), taken directly from NOAA Data.

Column O: Air Temperature (°C), the average of the daily high and low temperatures.

Column P: Incoming Solar Radiation (kcal/m^2/day), from Baker (1979):

$=(37+0.622*(1-C))/100*(2635.9-101.213*(0.03261*D-5.576)^2+1.4342*(0.03261*D-5.576)^4)*0.252/0.3048^2$

where C is the percent of cloud cover, and N is the Julian day. This formula is discussed in Section 7.3.3.1.

Column Q: Vapor Pressure of Air, ψE_a (mm Hg), from the Tennessee Valley Authority (1972):

$=EXP(2.3026*((7.5*T_d-236.9)/(T_d+395.5)+0.6609))$

where where T_d is the dewpoint temperature (°C).

Column R: Wind speed (m/sec), taken directly from NOAA data.

Column S: Percent of sun, which is (100-C), where C is percent of cloud cover.

Row 2:	From Column C to Column L, the elevation of the bottom of each layer (Column C is 0 m, Column L is 6.8577 m).
Row 4:	From Column C to Column L, the area of the bottom of each layer (m^2).
Row 5:	Initial temperatures for the model (in this case, on December 31st, all layers are 4.1°C).
Row 6 to	
Row 1469:	Data for each quarter day (Row 6 is quarter day 1, Row 1469 is quarter day 1464 (end of day 366)).

For Day 1 (Row 6), the following equations were used:

Bottom Layer Temperature = \$C5+(1/1000000/0.001/\$C\$4/2/0.762*(\$P6*0.55*EXP(-0.75*(\$L\$2-\$D\$2))*\$D\$4)+0.0001763/\$C\$4/2/0.762*((\$D5-\$C5)/0.762*\$D\$4))*0.25

Surface Layer Temperature =\$K5+(1/1000000/0.001/((\$K\$4+\$L\$4)/2)/0.762*(\$P6*0.55*\$L\$4-\$P6*0.55*EXP(-0.75*(\$L\$2-\$K\$2))*\$K\$4)-0.0001763/((\$K\$4+\$L\$4)/2)/0.762*((\$K5-\$J5)/0.762*\$K\$4)+1/1000000/0.001/((\$K\$4+\$L\$4)/2)/0.762*(0.45*\$P6*\$L\$4)-1/1000000/0.001/((\$K\$4+\$L\$4)/2)/0.762*\$L\$4*(0.97*0.00000171*((\$K5+273)^4-0.00000937*(\$O6+273)^6*(1+0.17*((100-\$S6)/100)^2))+(0.000308+0.000185*\$R\$6)*1000*(0.0003183*\$K5^3+0.01039*\$K5^2+0.31177*\$K5+4.619-\$Q6)*(595.9-0.54*(\$K5+273)+1*\$K5+269.1*(\$K5-\$O6)/(0.0003183*\$K5^3+0.01039*\$K5^2+0.31177*\$K5+4.619-\$Q6))))*0.25

Temperature for Layer 2 (Column D)
=D5+(1/1000000/0.001/((D\$4+E\$4)/2)/0.762*(\$P6*0.55*EXP(-0.75*(\$L\$2-E\$2))*E\$4-\$P6*0.55*EXP(-0.75*(\$L\$2-D\$2))*D\$4)+0.0001763/((D\$4+E\$4)/2)/0.762*((E5-D5)/0.762*E\$4-(D5-C5)/0.762*D\$4))*0.25

The formula for all intermediate layers (Column D to Column J) are copies of the one for 2D. The formulas for all quarter days (Rows 5 to 1469) are copies of the formulas above. Spreadsheet locations preceded by dollars signs (i.e. K6, K$6 or $K6) are absolute and do not change with copying. All spreadsheet locations without dollar signs are relative, and the distance of the location relative to the cell in which an equation is copied stays constant. For example, a formula in cell A1 copied to cell C6 would differ from the original in that all K6's would be changed to N12's, all K$6's to N$6's, and all $K6's to $K12's. All K6's would stay as K6's.

Though they may appear confusing, the formulas above are equivalent to equations 7-25 and 7-26. There are two numbers which must be changed if the model is used for another pond: the thickness of each layer (0.762 m for Snake Pond) and the extinction coefficient (0.75 m^{-1} for Snake Pond). The 0.25 days by which each formula is multiplied at the end may be changed if a different Δt is desired. Here are a couple of expressions that may not be obvious to the reader: (1/1000000/0.001/((K4+L4)/2)/0.762) equals $1/\rho c A_j \Delta y$, where A_j is the layer between Column K and Column L. In the surface layer, the expression (0.0003183*$K5^3+0.01039*$K5^2+0.31177*$K5+4.619-$Q6) is a best fit polynomial for the vapor pressure of water, given temperature $K5 (where $K5 is from the previous quarter day).

A.2 Visual Basic Macro

The SPTM macro recalculates the temperature profiles in the spreadsheet to account for mixing, and also calculates the depth to which wind mixing occurs. There is one formula in the macro which has not been discussed: The function **WaterDensity**, which depends on the water temperature, is a best fit polynomial from CRC (1990). The other formulas, as well as the theories behind wind and convective mixing, are described in Section 7.3.3.5 and 7.3.3.6.

The SPTM macro refers to the SPTM spreadsheet as *Sheet2*, so that *Sheet1* may hold an extra copy of the initial data. Once the macro has been run, the initial data must be recopied onto *Sheet2* before running again.

A.2.1 Convective Mixing Routine

The convective mixing routine (convective mixer) in the SPTM macro takes an unmixed temperature profile and mixes all layers whose densities make them unstable. The convective mixer takes a temperature profile and starts by comparing the two layers closest to the surface. If the density gradient is unstable, they are mixed, and both layers are given a temperature of T_{new}, as defined in equation 7-14. The mixer then looks at the second layer and the third layers from the surface, and repeats the process all the way to the bottom. At all times, the model keeps track of how many consecutive layers it has mixed. Whenever the mixer uses equation (7.x), it sets V_n equal to the volume of the lower layer and T_n as the temperature of the lower layer. But instead of mixing this layer with only the one layer directly above, it mixes it with all layers above it that had already been mixed. So V_m becomes the volume of all mixed layers above, and T_m becomes their temperature. (Since the layers above have all been mixed together, they are all at the same temperature.)

This procedure accurately mixes the pond, with fewer calculations than would be necessary if only two layers were mixed at a time. If such an algorithm were employed, the mixer would need to cycle from the surface to the bottom many times before all unstable density gradients were eliminated. However, the procedure employed by the SPTM convective mixer is not perfect. Since the convective mixer makes only one pass from the surface to the bottom of the pond, it may output unstable density gradients if temperatures at the bottom of the pond are erratic. The errors associated with this are on the order of 0.05°C, which are not considered significant to the predictive power of the model. However, unstable temperature profiles can affect the wind mixing routine, and some special commands have been inserted into the wind mixer to alleviate any potential problems. Section A.2.2 contains a more detailed discussion of the topic.

A.2.2 Wind Mixing Routine

To account for wind mixing, the SPTM has a wind mixing routine (wind mixer). The wind mixer begins by reading the temperatures generated by the convective mixer. The wind mixer mixes layer by layer, starting with the two layers closest to the surface. Mixing layer j with the layers above requires an amount of energy $PE_j/f(Ri)$, so this amount is subtracted from original KE. The wind mixer moves down to the next layer, and continues this process until there is not enough kinetic energy to mix any further. No layers are mixed if the temperature of the surface layer is less than zero (i.e., there is ice on the surface).

While the convective mixer is designed to remove all unstable temperature gradients, it only runs through the pond once, going from the surface to the bottom. Therefore, there may be small unstable density gradients which are not caught by the convective mixer. While these errors do not significantly effect to the predictive power of the model, they cause some mathematical problems within the wind mixer, which automatically assumes no unstable density gradients. To account for these errors, there are numerous checks within the wind mixer, which prevent the kinetic energy gained and the Richardson number from being less than zero, and keep f(Ri) from being less than or equal to zero. An f(Ri) value less than or equal to zero implies that the density profile is either somewhat unstable or extremely stable. A plot of the Richardson number vs. F(Ri) is shown in Figure A-1. Here, the Richardson number can be considered as a measure of the strength of stratification. If f(Ri) is initially calculated to be non-positive, the model pushes up the value of f(Ri) to 0.00001. If the profile is unstable, the PE calculated is zero and the layers mix with no loss or gain of KE. If it is stable, the low value of f(Ri), along with the large value of PE prevent layers from mixing.
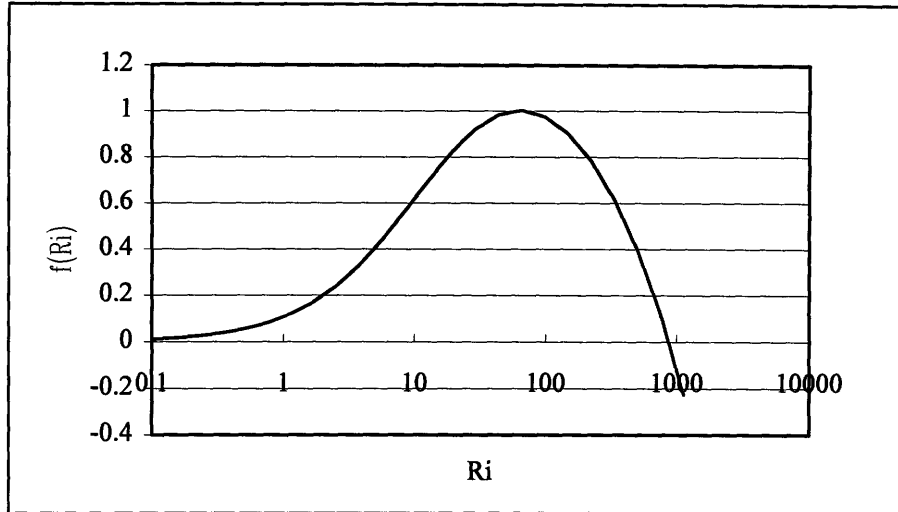
Figure A-1: Relationship of f(Ri) to Ri

A.3 Using the SPTM for Other Ponds

The SPTM spreadsheet can be modified for use in modeling other ponds, as long as the assumptions described in Section 7.3.2 remain valid. There is room within the sheet to handle up to 10 pond layers. If the pond is divided into more than 10 layers, some changes within both the spreadsheet and the marco are necessary.

To add layers, extra spreadsheet columns should be inserted between the fourth and fifth layers from the bottom. Excel will automatically change all variables within the formulas, so that they point to the right cell. Then the appropriate layer areas and elevations should be entered, and the formula for Column D, Row 6 (given in Section A.1) should be copied and pasted to all the extra layers. (It is not important where the columns are inserted, as long as they are somewhere between the layers, at least two layers away from the surface and three away from the bottom. Otherwise the molecular diffusion may bypass a layer.)

Some modifications to the macro must be made as well. Each pond will have differerent values for **n** (the number of layers) and **deltaY** (the thickness of each layer), and these should be entered into the macro. If more than 10 layers are used, the two lines in the macro which read in spreadsheet values for **AirPressure** and **AirVP** should be modified so that they point to the proper cells.

A.3 The Macro Code

```
Sub Mixer()

'General Variables
    Dim Pointer As Integer      'Keeps track of the top of the mixed
                                'layer
    Dim x As Integer            'Generic Counter Variable
    Dim Layer As Integer        'Keeps track of the layer to be mixed
    Dim Temp(9) As Single       'Temperature of each layer (C)
    Dim Day As Integer          'Day of the year (Quarter Days)
    Dim MixArea As Single       'Integral of A * dz / Mixing Height (m2)
    Dim MixTemp As Single       'Integral of T * dz / Mixing Height (C)
    Dim Area(10) As Single      'Area of each layer, and the surface
                                'area (m2)
    Dim n As Single             'Number of layers

'Wind Mixing Variables
    Dim WindSpeed As Single     'Wind speed, read from spreadsheet
                                '(m/sec)
    Dim AirPressure As Single   'Air pressure, read from spreadsheet (mm
                                'Hg)
    Dim deltaY As Single        'Thickness of layers (m)
    Dim AirVP As Single         'Air vapor pressure, read from
                                'spreadsheet (mm Hg)
    Dim AirDensity As Single    'Density of air (kg/m3)
    Dim Density1 As Single      'Density of last layer mixed (kg/m3)
    Dim Density2 As Single      'Density of layer to be mixed (kg/m3)
    Dim KE As Single            'Kinetic Energy (N-m)
    Dim PE As Single            'Potential Energy of Mixing (N-m)
    Dim Ri As Single            'Richardson Number
    Dim fRi As Single           'f(Ri) = Ratio of PE gained to KE lost, if two
                                'layers mix
    Dim Gravity As Single       'Gravity (9.8m/s2)
    Dim WindMixElevation As Single   'Depth to which the wind mixes
                                     '(expressed as meters from the
                                     ' bottom of the pond)

'Reads in Areas of layers, start of the Day counter
```

```
    n = 9
    For x = 1 To 10
        Area(x) = Worksheets("Sheet2").Cells(4, x + 2).Value
    Next x


    For Day = 1 To 1464
        For x = 1 To n
            Temp(x) = Worksheets("Sheet2").Cells(Day + 5, x + 2).Value
        Next x

' Convective Mixer

        Pointer = n
        For Layer = n To 2 Step -1
            Density1 = WaterDensity(Temp(Layer))
            Density2 = WaterDensity(Temp(Layer - 1))
            If Density1 > Density2 Then
                MixArea = 0
                For x = Layer To Pointer
                    MixArea = MixArea + Area(x)
                Next x
                If Layer > 2 Then
                    Temp(Layer - 1) = (MixArea * Temp(Layer) + _
            Temp(Layer - 1) _
                        * Area(Layer - 1)) / (MixArea + Area(Layer - 1))
                Else Temp(Layer - 1) = (MixArea * Temp(Layer) +
            Area(Layer - 1) / _
                2 * Temp(Layer - 1)) / (MixArea + 1 / 2 * Area(Layer - 1))
                End If
                For x = Layer To Pointer
                    Temp(x) = Temp(Layer - 1)
                Next x
            Else Pointer = Layer - 1
            End If
        Next Layer

' Wind Mixer

        if temp(9) > 0 then
            deltaY = 0.762
            WindSpeed = Worksheets("Sheet2").Cells(Day + 5, 18).Value
            AirVP = Worksheets("Sheet2").Cells(Day + 5, 17).Value
            AirPressure = Worksheets("Sheet2").Cells(Day + 5, 14).Value
```

```
AirTemp = Worksheets("Sheet2").Cells(Day + 5, 15).Value
AirDensity = 1.2929 * (273.13 / _
        (AirTemp + 273.13)) * (AirPressure - 0.3783 * AirVP) / 760
Layer = n
Pointer = n
Gravity = 9.81
Density1 = WaterDensity(Temp(Layer))
Density2 = WaterDensity(Temp(Layer - 1))
Ri = Gravity * (Density2 - Density1) * deltaY / _
      (0.001 * AirDensity * WindSpeed ^ 2)
If Ri < 0 Then Ri = 0
fRi = 0.057 * Ri * ((29.5 - Ri ^ 0.5) / (14.2 + Ri))
If fRi = 0 Then fRi = 0.0001
PE = Area(Layer) * deltaY * (Density2 - Density1) * Gravity * _
      ((10 - Layer) * deltaY) / 2
If PE < 0 Then PE = 0
KE = Area(10) * 0.25 * ((1 + 0.05 * WindSpeed ) * 0.001 * AirDensity * _
        WindSpeed ^ 2) ^ (3 / 2) _
      / (Density1 ^ 0.5) * 24 * 3600
While (KE > PE / fRi) And (Layer > 1)
    MixArea = 0
    For x = Layer To Pointer
        MixArea = MixArea + Area(x)
    Next x
    If Layer > 2 Then
        Temp(Layer - 1) = (MixArea * Temp(Layer) + _
                Temp(Layer - 1) * _
            Area(Layer - 1)) / (MixArea + Area(Layer - 1))
    Else Temp(Layer - 1) = (MixArea * Temp(Layer) + _
            Area(Layer - 1) / _
        2 * Temp(Layer - 1)) / (MixArea + 1 / 2 * _
          Area(Layer - 1))
    End If
    For x = Layer To Pointer
        Temp(x) = Temp(Layer - 1)
    Next x
    KE = KE - PE / fRi
    Layer = Layer - 1
    Density1 = WaterDensity(Temp(Layer))
    Density2 = WaterDensity(Temp(Layer - 1))
    Ri = Gravity * (Density2 - Density1) * deltaY / _
          (0.001 * AirDensity * WindSpeed ^ 2)
    If Ri < 0 Then Ri = 0
```

```
            fRi = 0.057 * Ri * ((29.5 - Ri ^ 0.5) / (14.2 + Ri))
            PE = Area(Layer) * deltaY * (Density2 - Density1) * _
                    Gravity * ((10 - Layer) * deltaY) / 2
            If Layer = 2 Then PE = PE / 2
            If PE < 0 Then PE = 0
            If fRi = 0 Then fRi = 1
        Wend
    End If
    If Layer > 1 Then
        WindMixElevation = (Layer - KE / (PE / fRi)) * deltaY
    Else WindMixElevation = 0
    End If


' Return Values to Spreadsheet, Calculates Next Day

    For x = 1 To n
        Worksheets("Sheet2").Cells(Day + 5, x + 2).Value = Temp(x)
    Next x
    Worksheets("Sheet2").Cells(Day + 5, n + 3).Value _
            = WindMixElevation
    Worksheets("Sheet2").Rows(Day + 6).Calculate
    Next Day
End Sub



Function WaterDensity(Temperature)
    WaterDensity = (999.83952 + 16.945176 * Temperature - _
    0.0079870401 * Temperature ^ 2 _
    - 0.000046170461 * Temperature ^ 3 + 0.00000010556302 * _
    Temperature ^ 4 + 0.000000000410411 * Temperature ^ 5) / _
    (1 + 0.01687985 * Temperature)
End Function
```

Appendix B: The Head-Calculating Macro and Formula for Streamlines

B.1 The Head-Calculating Macro

In order to calculate a two-dimensional plot of head over the FS-12 area, a Visual Basic macro was created. This macro creates a grid of data, the resolution of which is defined by the user, in XYZ format. That is, the x-axis (easting) is put in column A, the y-axis (northing) in column B, and the z-axis (head) in column C. This format was used to facilitate use in advanced graphing programs such as SURFER.

The head-calculating macro starts by reading in all data from the sheet named *Formatted*, and initializes its counters. To calculate head, equation 4-8 was employed, with the sum of well influences calculated in a for/next loop. It then outputs the data to a separate sheet named *Grid*. It first calculates over the entire FS-12 area at a low resolution (defined by the user) and then calculates regions near the wells at a higher resolution (1 point per square foot). At a resolution of 1 point per 20 feet, the macro requires more than the 16354 rows allowed by Excel. The macro has been designed to continue wrapping data to the next three columns, until all calculations are completed.

```
Sub HeadCalculation()
    Dim Resolution As Integer
    Dim x As Single
    Dim y As Single
    Dim Gx As Single
    Dim Gy As Single
    Dim K As Single
    Dim b As Single
    Dim w As Single
    Dim Xupper As Single
    Dim Xlower As Single
    Dim Yupper As Single
    Dim Ylower As Single
    Dim Xi(53) As Single
    Dim Yi(53) As Single
    Dim Head As Single
```

```
    Dim Flow(53) As Single
    Dim Counter As Integer
    Dim Well As Integer
    Dim Count2 As Integer
    Dim Count3 As Integer


For Counter = 1 To 53
    Xi(Counter) = Worksheets("Formatted").Cells(Counter + 1, 2).Value
    Yi(Counter) = Worksheets("Formatted").Cells(Counter + 1, 3).Value
    Flow(Counter) = Worksheets("Formatted").Cells(Counter + 1, 4).Value
Next Counter


K = Worksheets("Formatted").Cells(1, 7).Value
b = Worksheets("Formatted").Cells(2, 7).Value
w = Worksheets("Formatted").Cells(3, 7).Value
Gx = Worksheets("Formatted").Cells(4, 7).Value
Gy = Worksheets("Formatted").Cells(5, 7).Value
Resolution = Worksheets("Formatted").Cells(6, 7).Value
Xlower = Worksheets("Formatted").Cells(7, 7).Value
Xupper = Worksheets("Formatted").Cells(8, 7).Value
Ylower = Worksheets("Formatted").Cells(7, 8).Value
Yupper = Worksheets("Formatted").Cells(8, 8).Value
Count2 = 0
Count3 = 0


For x = Xlower To Xupper Step Resolution
    For y = Ylower To Yupper Step Resolution
        Count2 = Count2 + 1
        Head = Gx * x + Gy * y
        For Counter = 1 To 53
            If ((x - Xi(Counter)) ^ 2 + (y - Yi(Counter)) ^ 2) < 1000 Then _
            Head = Head + Flow(Counter) / 4 / 3.141 / K / b * Log(((x + 0.5 -
Xi(Counter)) ^ 2 + (y + 0.5 - Yi(Counter)) ^ 2) ^ 0.5 / 1000)
        Next Counter
        If Count2 > 16384 Then
            Count2 = 1
            Count3 = Count3 + 1
        End If
        Worksheets("Grid").Cells(Count2, 1 + Count3 * 3).Value = x
        Worksheets("Grid").Cells(Count2, 2 + Count3 * 3).Value = y
        Worksheets("Grid").Cells(Count2, 3 + Count3 * 3).Value = Head
    Next y
Next x


For Well = 1 To 53
    For x = (Xi(Well) - 10) To (Xi(Well) + 10) Step 1
        For y = (Yi(Well) - 10) To (Yi(Well) + 10) Step 1
        Head = Gx * x + Gy * y
        For Counter = 1 To 53
            If ((x - Xi(Counter)) ^ 2 + (y - Yi(Counter)) ^ 2) < 1000 Then _
            Head = Head + Flow(Counter) / 4 / 3.141 / K / b * Log(((x + 0.5 -
Xi(Counter)) ^ 2 + (y + 0.5 - Yi(Counter)) ^ 2) ^ 0.5 / 1000)
```

```vbnet
        Next Counter
        If Count2 > 16384 Then
            Count2 = 1
            Count3 = Count3 + 1
        End If
        Worksheets("Grid").Cells(Count2, 1 + Count3 * 3).Value = x
        Worksheets("Grid").Cells(Count2, 2 + Count3 * 3).Value = y
        Worksheets("Grid").Cells(Count2, 3 + Count3 * 3).Value = Head
        Next y
    Next x
Next Well
End Sub
```

B.2 The Streamline Function

In order to calculate the streamlines, a derivation for the streamfunction was attempted. However, due to a discontinuity in the final derived equation, streamlines were approximated using the head equation and drawing in orthogonal lines. Starting from equation 4-8, the seepage velocity v can be determined using the gradient of the head. Differentiating and rearranging terms gives

$$v = \frac{T}{b\varpi}\nabla h = \{\frac{Tg_x}{b\omega} + \sum_{i=1}^{n}\frac{Q_i(x - x_i)}{4\pi b\omega[(x - x_i)^2 + (y - y_i)^2]}\}\hat{i}$$
$$+ \{\frac{Tg_y}{b\omega} + \sum_{i=1}^{n}\frac{Q_i(y - y_i)}{4\pi b\omega[(x - x_i)^2 + (y - y_i)^2]}\}\hat{j}$$

Eq. B-1

where i and j are unit vectors in the x and y directions respectively.

By obtaining the stream function for the aquifer, it is possible to see where the reinjected water flows. The stream function ψ is defined so that

$$v_x = \frac{\partial\psi}{\partial y} \quad \text{and} \quad v_y = -\frac{\partial\psi}{\partial x}$$

Eq. B-2, 3

where v_x and v_y are the x and y components of the seepage velocity respectively. Two points with equal values for the stream function lie along the same flowline.

The stream function can be obtained by integrating the y-component of equation B-1:

$$\frac{\partial\psi}{\partial y} = \frac{Tg_x}{b\omega} + \sum_{i=1}^{n}\frac{Q_i(x - x_i)}{4\pi b\omega[(x - x_i)^2 + (y - y_i)^2]}$$

Eq. B-4

using the integral

$$\int \frac{du}{a^2 + u^2} = \frac{1}{a} \tan^{-1}(\frac{u}{a})$$

Eq. B-5

we get

$$\psi = \frac{Tg_x y}{b\omega} + \sum_{i=1}^{n} \frac{Q_i}{4\pi b\omega} \tan^{-1}(\frac{y - y_i}{x - x_i}) + f(x)$$

Eq. B-6

where $f(x)$ is some function of x, which can be solved by differentiating the stream function with respect to y, and substituting into equation B-11. If we let

$$a = \frac{1}{y - y_i} \quad \text{and} \quad u = \frac{1}{x - x_i}$$

Eq. B-7, 8

and use equation B-5 again, we get

$$\frac{\partial \psi}{\partial x} = \sum_{i=1}^{n} \frac{Q_i a}{4\pi b\omega} [\frac{1}{a^2 + u^2}](\frac{du}{dx}) + f'(x)$$

$$= \sum_{i=1}^{n} \frac{-Q_i(y - y_i)}{4\pi b\omega} [\frac{1}{(x - x_i)^2 + (y - y_i)^2}] + f'(x)$$

Eq. B-9

Equating equation B-9 to -v_y, we find that

$$f(x) = -\frac{Tv_y x}{b\omega}$$

Eq. B-10

and so the stream function is

$$\psi = \frac{T}{b\omega}(v_x y - v_y x) + \sum_{i=1}^{n} \frac{Q_i}{4\pi b\omega} \tan^{-1}(\frac{y - y_i}{x - x_i})$$

Eq. B-11

Attempts to apply equation B-11 to the FS-12 area do not yield reasonable results. While the formula works well in describing streamlines for a single well (see Figure B-1), there is a discontinuity associated with the inverse tangent function (Figure B-2) which causes sudden jumps in streamlines crossing the x-coordinate of a well.
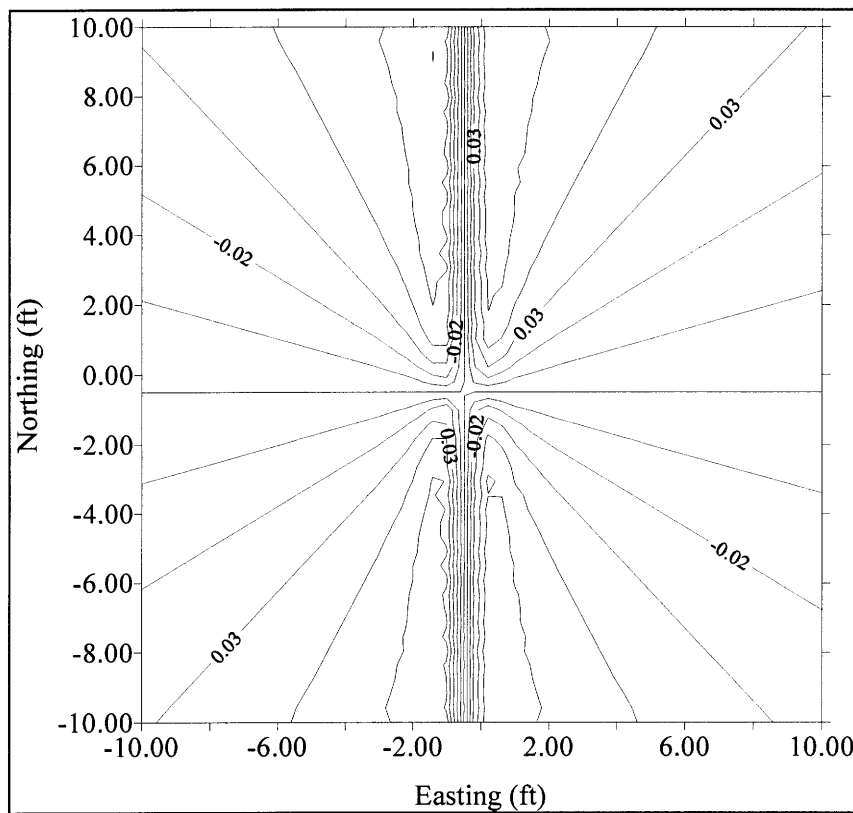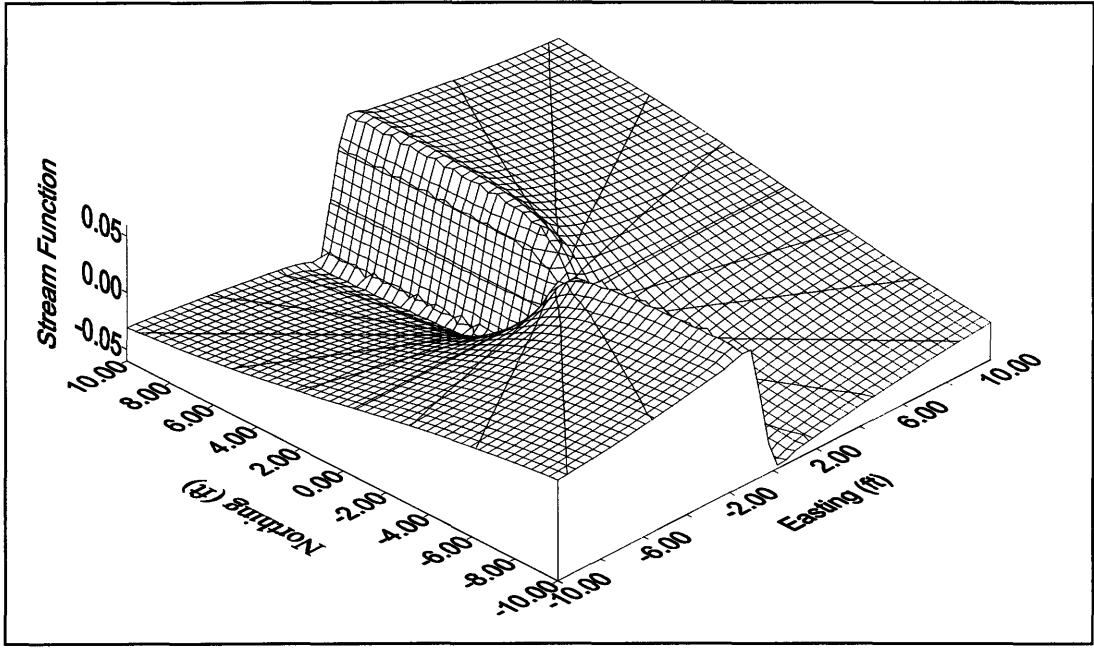

Figure B-1: Stream Function Contours for One Well

Figure B-2: Surface Map of Stream Function